Université de Montréal

The effect of calcium homeostasis on HSV-1 propagation

Par

Mayerline Dorsainvil

Département de Microbiologie, Infectiologie et Immunologie

Faculté de Médecine

Mémoire présenté en vue de l'obtention du grade de Maitrise ès Science (M.Sc.)

en Microbiologie et Immunologie

19 Janvier, 2020

Université de Montréal

Département de Microbiologie, Infectiologie et Immunologie, Faculté de Médecine

---

Ce mémoire intitulé

The effect of calcium homeostasis on HSV-1 propagation

Présenté par

Mayerline Dorsainvil

A été évalué par un jury composé des personnes suivantes

Guy Lemay

Président-rapporteur

Roger Lippé

Directeur de recherche

Louis-Éric Trudeau

Membre du jury

Résumé

Au cours d'une infection lytique, le virus de l'herpès simplex de type 1 (VHS-1) doit entreprendre plusieurs étapes de fusion afin de se répliquer et se propager correctement. Ainsi, le virus a évolué afin de tirer avantage de la machinerie cellulaire en utilisant des protéines et facteurs de l'hôte à cet effet. Dans la littérature, les processus sous-jacents à l'entrée du VHS-1 ont été largement élucidés. Cependant, on ne sait toujours pas comment les particules virales nouvellement synthétisées sortent de la cellule hôte et quels facteurs cellulaires sont impliqués dans ce processus. Des résultats publiés par notre laboratoire indiquent que la protéine cellulaire, Extended Synaptotagmin 1 (E-Syt1), a un impact négatif sur la propagation globale du virus lorsqu'inhibée par de l'ARN d'interférence. Conséquemment, la présente étude a pour objectif de confirmer et d'approfondir le rôle d'E-Syt1 sur la propagation virale, en particulier sur la sortie du virus. Étant donné que l'activation d'E-Syt1 est liée à l'augmentation de la concentration de calcium cytoplasmique, nous avons également étudié l'implication du calcium au cours des stades ultérieurs de la réplication virale. Ici, nous avons démontré que la surexpression d'E-Syt1 n'a pas d'effet détectable sur la sortie du VHS-1, mais que le calcium a effet sur la propagation virale. Alors que la séquestration précoce du calcium (4 et 6 heures post-infection) à l'aide de chélateurs réprime la sortie virale, aucun effet significatif a été détecté lorsque les chélateurs ont été ajoutés à un stade avancé de l'infection (12 et 16 heures post-infection). Nos résultats fournissent des données intéressantes sur la nécessité de l'homéostasie du calcium intracellulaire afin que VHS-1 puisse assurer une médiation adéquate de la sortie virale. Ces résultats pourraient conduire à la découverte de nouveaux mécanismes ou protéines cellulaires régulées par le calcium et utilisés par le VHS-1 lors de réplications lytiques virales.

Mots-clés : VHS-1, sortie virale, calcium, stade d'infection, E-Syt1

Abstract

During a lytic infection, Herpes Simplex Virus type 1 (HSV-1) must go through multiple steps of fusion to replicate and propagate properly. For this purpose, the virus has evolved consequently by taking advantage of the cellular machinery using host factors and proteins. In the literature, processes underlying HSV-1's entry have been extensively elucidated. However, it remains unclear how newly synthesized viral particles egress from the host cell, and what cellular factors are implicated in this process. Results published by our laboratory suggest that the cellular protein, Extended Synaptotagmin 1 (E-Syt1), has a negative and global impact on the viral propagation when down regulated by RNA interference. Consequently, this study aims to confirm and deepen our understanding of E-Syt1's role on HSV-1, particularly during viral egress. Since activation of E-Syt1 is linked to the increase in cytoplasmic calcium concentration, we also investigated calcium involvement during later stages of viral propagation. Interestingly, overexpression of E-Syt1 had no measurable effect on HSV-1 propagation whereas calcium has a dual effect on viral propagation. While early calcium sequestering (4 and 6 hours post-infection) using chelators represses viral egress, no significant effect was detected when chelators were added at later time points (12 and 16 hours post-infection). Our results give interesting insights on how HSV-1 relies on intracellular calcium homeostasis to properly mediate viral egress. These results may lead to the discovery of new mechanisms or cellular proteins that are regulated by calcium and hijacked by HSV-1 during lytic replication.

Keywords: HSV-1, viral egress, calcium, time points, E-Syt1

Table of Contents

Résumé i
Abstract ii
Table of Contents iii
List of Figures v
List of Tables vi
List of Abbreviations vii
Acknowledgements x
1. Introduction 1
1.1. HSV-1 Structure 2
1.2. Viral Entry 3
1.3. Nuclear Entry 6
1.4. Viral Genomic Expression and Replication 7
1.5. Capsid Assembly and DNA Packaging 9
1.6. Nuclear Egress 9
1.7. Tegumentation and Re-Envelopment 11
1.8. Cell-to-Cell Spread 12
1.9. gM and E-Syt 1 Interaction 12
1.9.1. E-Syt1 13
1.9.2. E-Syt1 Structure 14
1.9.3. E-Syt1 Activation 16
1.10. Calcium and HSV-1 17
1.11. Hypothesis and Approach 17
2. Material and Methods 18
2.1. Cell line 18
2.2. Viruses and Infection 18
2.2.1. HSV-1 17+ WT 18
2.2.2. HSV-1 V701 19
2.2.3. HSV-1 K26 GFP 19
2.3. Plasmids 20

2.3.1. EGFP E-Syt1 WT, mCherry E-Syt1 (7x) and EGFP E-Syt1 ΔC2E constructs. 20
2.3.2. EGFP-N2 21
2.3.3. pCyto-gBFull 21
2.4. Transfection 22
2.5. Plaque Assay 22
2.6. Western Blot 23
2.7. Drugs 23
2.8. Immunofluorescence 23
2.9. qPCR 24
2.9.1. Infectivity ratio 24
2.10. Viability test 25
2.10.1. Drugs 25
2.10.2. Transfection 25
2.11. Statistics 25
3. Results 26
3.1. Calcium is required for HSV-1 egress 26
3.2. Calcium Is Required at Early Time Points During HSV-1 Egress 30
3.3. Chelation of Intracellular Calcium Early During Viral Egress Reduces Viral Genomic DNA Replication 33
3.4. Mutants of E-Syt1 Do Not Induce Viral Titer Recovery 39
4. Discussion 45
5. Conclusion 49
6. Bibliography 50

List of Figures

Fig 1. The structure of HSV-1's genome 2
Fig 2. The two models of HSV-1 entry inside a cell 5
Fig 3. Structure of E-Syt1 and mutations used in this study 15
Fig 4. Hela cell viability is not affected by the different calcium chelators or ionomycin treatments 27
Fig 5. Chelation of intracellular calcium inhibits viral egress 28
Fig 6. Viral localization inside the cell is not affected by post entry calcium level changes 29
Fig 7. The viral titer is decreased in the supernatant when cytosolic calcium is chelated at early time point during viral egress 32
Fig 8. The viral titer is decreased in the cell lysate when cytosolic calcium is chelated at early time point during viral egress 33
Fig 9. Chelation of cytosolic calcium reduces the amount of newly synthesized viral DNA in the supernatant 35
Fig 10. Chelation of cytosolic calcium reduces the amount of newly synthesized viral DNA in the cell lysate fraction 36
Fig 11. Changes in the cytosolic calcium level affect the infectivity ratio of newly synthesized viral particles released in the supernatant 37
Fig 12. Changes in the cytosolic calcium level affect the infectivity of newly synthesized viral particles released in the cell lysate fraction 38
Fig 13. Overexpression of the different constructs of E-Syt1 does not affect cell viability .. 41
Fig 14. The different E-Syt1 constructs are expressed at similar level 42
Fig 15. Overexpression of the different E-Syt1 mutants did not inhibit viral egress in the supernatant of infected Hela cells 43
Fig 16. Overexpression of the different E-Syt1 mutants did not inhibit viral egress in the cell lysate of infected Hela cells 44

List of Tables

Table 1. Primer sequences used to remove the stop codon in mCherry E-Syt1 (7x) protein....21

List of Abbreviations

HSV-1: Herpes simplex virus type 1

E-Syt1: Extended-Synaptotagmin 1

E-Syt2: Extended-Synaptotagmin 2

E-Syt3: Extended-Synaptotagmin 3

Syt: Synaptotagmin

Tcb: Tricalbin

AD: Alzheimer's disease

TNF: Tumour necrosis factor

U_L: Long unique sequence

U_S: Short unique sequence

$IR_{L:}$ Internal long repeat

$TR_{L:}$ Terminal long repeat

$IR_{S:}$ Internal short repeat

$TR_{S:}$ Terminal short repeat

TGN: Trans-Golgi network

gB: Glycoprotein B

gC: Glycoprotein C

gD: Glycoprotein D

gH: Glycoprotein H

gL: Glycoprotein L

gM: Glycoprotein M

gN: Glycoprotein N

HVEM: Herpesvirus entry mediator

HS: heparan sulfate

3-O-HS: 3-O sulfated heparan sulfate

PM: Plasma membrane

ER: Endoplasmic reticulum

NMHC-IIA: non-muscle myosin heavy chain IIA

NMHC-IIB: non-muscle myosin heavy chain IIB

MT: Microtubule

NM: Nuclear membrane

INM: Inner nuclear membrane

ONM: Outer nuclear membrane

NCP: Nuclear pore complex

Nup: Nucleoporin

HCF1: Host cell factor 1

Oct1: Octamer-binding protein 1

H/P: Helicase/primase complex

ssDNA: single-stranded DNA

dsDNA: double-stranded DNA

SERCA: Sarco/endoplasmic reticulum Ca2+ ATPase

PMCA: Plasma membrane Ca2+ ATPase

SMP: Synaptotagmin-like mitochondrial lipid-binding protein

$PI(4,5)P_2$: Phosphatidylinositol-4,5-bisphosphate

PLC: Phospholipase C

IP_3: Inositol triphosphate

DAG: Diacylglycerol

IP_3-R: IP_3-receptor

SOCE: Store-operated Ca^{2+} entry

PAA: phosphonoacetic acid

IFN: Interferon

Mayerline Dorsainvil

Acknowledgements

First, I would like to thank my family who supported me throughout the realization of my master's degree. They were present during the highs and lows, and always believed in me and my abilities to make great achievements.

Second, I would like to thank my colleagues from the laboratory who are now great friends. Without their helps, advice, opinions, knowledge and amazing energy, I would not have been able to finish my master's degree. Bita, Mackenzie, Hugo, Elisabeth, Catherine and Kendra, I will be forever grateful that I had the chance to work with such great individuals and scientists. Also, a special thanks for the students in Michel Desjardin's laboratory, Melanie and Ahmed, who were always there to help me in my experiments.

Third, I would like to thank Johanne for her amazing work as a lab technician. Her devotion to her work and making sure that the lab runs properly was remarkable. Not only my project, but the projects of everyone in the lab were successful because of you. Thank you so much! And for Marie-Josée who takes over so graciously after Johanne's retirement, I would like to express my sincere appreciation. You always had a positive energy and ready to overcome any challenges. Thank you for your help and support.

Last but not least, I would like to thank the principal investigator of my laboratory, Dr. Roger Lippé. You gave me the chance to work in your laboratory and bloom as the scientist that I am today. Your door was always open when I needed a second look at my results and you always supported me with my thousands of ideas for this project. I will also like to thank you for making sure that there was always a great atmosphere in the lab by encouraging us to make activities (sport, restaurants, etc.) together. Maybe someday I will be as good as you in squash, and I'll be able to get revenge. It was my pleasure and honour to work with you and I wish you all the best for the lab at Ste-Justine.

1. Introduction

Herpesviridae is a large family of DNA viruses that subdivide into three subgroups; Alphaherpesvirinae, Betaherpesvirinae and Gammaherpesvirinae [1]. Viruses from these three groups have a broad tropism and can infect human and different species of animals. Beta- and Gammaherpesvirinae are comprised of 18 and 32 species of viruses respectively, whose diseases cause mild to severe symptoms, and even death [1, 2]. Viruses like HHV-5 (human cytomegalovirus), HHV-6 (sixth disease), HHV-4 (mononucleosis) and HHV-8 (Kaposi's sarcoma) are all examples of viruses that belong to those two subclasses [2]. Among all the 37 species of Alphaherpesvirinae, HHV-1 (herpes simplex virus 1), HHV-2 (herpes simplex virus 2) and HHV-3 (Varicella-Zoster virus) are examples of viruses commonly found in the human population. Indeed, it is estimated that 69% (3.7 billion individuals) of the world population is infected with herpes simplex virus type 1 (HSV-1) [3]. This widely spread infection is partly due to the fact that HSV-1 is asymptomatic. Additionally, this virus, as other Herpesviridae, has the capacity to go into latency. For HSV-1, the tropism for latency are trigeminal ganglions (TG) and the central nervous system (CNS) of the infected organism which lead to a lifelong persistent viral reservoir [4, 5]. HSV-1 transmission between organisms occurs through direct contact with the buccal mucosa, skin with or without lesions and genitals. It is important to mention that even during the asymptomatic period, the virus is still infectious as it can replicate and generate a small viral load in the infected individual. During a lytic viral replication, HSV-1 can cause painful open sores around the mouth, nose, face and inside the throat, but it can also cause keratitis in immunocompromised individuals and encephalitis in newborns [6-8]. Recently, it was suggested that brain damages caused by HSV-1 can lead to the development of neurodegenerative diseases like Alzheimer's disease (AD) [9, 10]. Furthermore, some studies demonstrated that patients who have oral submucous fibrosis, oral leukoplakia and other oral cancers also had a high cell-mediated immune response against HSV-1 [11-13]. In this context, it is clear that HSV-1 can lead to severe health issues, reinforcing the relevance of research aiming to understand cellular and molecular processes underlying HSV-1 propagation.

1.1. HSV-1 Structure

HSV-1 is an enveloped virus containing a 152 kbp linear double-stranded DNA genome [14]. The genome structure is composed of one long unique sequence (U_L) and one short unique sequence (U_S) [15] (figure 1). Both sequences are flanked by inverted repeats which allow the unique sequences to change orientation during DNA replication. Those inverted repeats are termed internal and terminal long repeats (IR_L, TR_L) or internal and terminal short repeats (IR_S, TR_S) (figure 1). Consequently, there are four possible genome orientations that are found in a pool of virus which all seems to be equally infectious [16, 17]. In the virus, essential genes responsible for lytic replication, DNA splicing and packaging are highly conserved [18]. At the IR_L and TR_L sequences, we find the LAT gene along with the RL1 and RL2 genes encoding for ICP0 and ICP34.5 respectively [19]. While the LAT gene encodes for latency-promoting micro RNAs, ICP0 and ICP34.5 are both implicated in early phases of the viral replication [17]. Similarly to the long repeats, IR_S and TR_S contain a highly conserved gene, RS1, which encodes for ICP4. ICP4 is also implicated in the early stages of viral replication as it regulates viral transcription [20]. Since both pairs of repeats have identical sequences, those four genes are present twice in the viral genome. The other 76 genes of HSV-1 are located throughout the U_L and Us sequences [21].

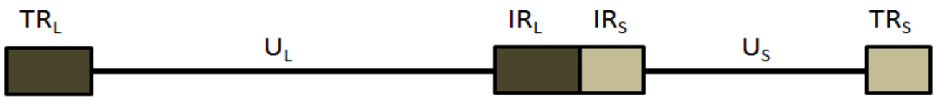

Fig 1. The structure of HSV-1's genome

This figure is from a recent publication [22]. The genome structure of HSV-1 is composed of a unique long and unique short sequences (U_L and Us) flanked by inverted repeats termed terminal and internal long repeats (TR_L and IR_L) and terminal and internal short repeats (TR_S and IR_S).

During capsid assembly and maturation, this large genome is tightly packed into the mature viral capsid. Capsids are mainly composed of four viral proteins that are highly organized to form the 20 faces of the capsid [23]. Each capsomer is composed of five or six monomers of VP5 linked to six monomers of VP26. Attached to the capsomers, there is a

heterotrimeric complex composed of two monomers of VP23 and one molecule of VP19C [24, 25]. Altogether, they form the 1250Å diameter icosahedral capsid [25]. Surrounding the nucleocapsid, there is a layer of tegument proteins required in many steps throughout the viral propagation. It is unclear where this layer of viral protein is added to the nucleocapsid, but some studies suggested that it mostly occurs as the viral particle pass through the trans-Golgi networks (TGN) and its interaction with endosomes containing tegument proteins [26-29]. To this day, there are about 20 viral proteins that were identified at the tegument, as well as some host cell proteins. As an example, VP1/2, also referred to as pU_L36, is an essential tegument protein at the early stage in the infection as it regulates DNA release from the incoming capsid inside the nucleus. A mutant virus lacking this tegument protein shows a significant decrease in *de novo* viral synthesis [30]. Other viral proteins like VP11, VP12, VP13/14, VP16, VP22 or pU_L37 have been identified as tegument proteins where their mutation affects viral propagation at different levels [31-33]. The final layer is composed of a host-derived phospholipid bilayer containing multiple glycoproteins implicated in cellular trafficking. Trafficking in the cell implies multiple steps of envelopment and de-envelopment which are tightly regulated by the fusion machinery mainly composed of glycoproteins B, D and H/L [34-36].

1.2. Viral Entry

Virus trafficking starts by the binding of the viral particle to the cell surface. Reversible bindings occur between viral glycoproteins and specific cellular receptors. Depending on the cell type, different glycoprotein-receptor interactions are required to enable an effective infection. HSV-1 primary infection site occurs at the mucosal epithelium where the viral glycoprotein B and C (gB and gC) interacts with cellular heparan sulfate (HS) [37]. This interaction enables docking of viral particles but is not sufficient to initiate penetration inside the cell [38]. Following this first interaction, the glycoprotein D (gD) interacts with one of the three possible cellular receptors: herpesvirus entry mediator (HVEM) which is part of the tumour necrosis factor (TNF) family, Nectin-1 or 2 and 3-O sulfated heparan sulfate (3-O-HS). They are all expressed by multiple types of human cells and are required to initiate fusion between the viral particle and the cell plasma membrane (PM) [39]. It was demonstrated that deleterious mutation affecting either one of those gD-receptor interactions significantly affects viral entry without completely abrogating it [40]. This suggests that HSV-1 uses redundant

mechanisms to ensure optimal viral entry. The glycoprotein complex H and L (gH/gL) was also reported to be involved in viral entry [41]. In fact, gH/gL interacts with integrin αVβ3, which was demonstrated to relocate nectin-1 to lipid rafts when overexpressed in cells [42]. Furthermore, one group suggested that gH acts as an activator of gB by binding to it through its domain III to support gB fusogenic activity [43]. Even if gH/gL functions are not clear, it seems to enhance viral entry efficiency. Since HSV-1 entry requires interaction with multiple receptors, it was reported that it occurs at receptor-rich sites (entry hotspot). Some studies demonstrated that gB can also interact with non-muscle myosin heavy chain IIA and B (NMHC-IIA or –IIB), which are receptors and motor proteins that allow the movement on actin filaments [44]. Since the plasma membrane is lined with a layer of cortical actin meshwork, gB-NMHC-IIA or -IIB interactions mediate viral particles to "surf" on the cell surface to reach those entry hotspots [45, 46]. Even if NMHC-IIA and -IIB are mostly expressed in the cytoplasm, exposure of HSV-1 to cells triggers the relocation of those motor proteins at the PM, especially at filopodia [44, 46].

Currently, there are two models describing HSV-1 entry into targeted cells (figure 2). It is important to mention that the type of entry depends on the cell line. In fact, HSV-1 enters Vero or HEp-2 cells by fusion with their PM while it enters Hela, epithelial or keratinocyte cells through a phagocytosis-like mechanism [47, 48]. The first model is the fusion of HSV-1 envelope with cellular PM. In this model, gB, gD, gH/gL are required to support the fusion between the two lipid bilayers [49]. The capsid and tegument proteins are directly released in the cytoplasm where most teguments detach from the capsid except VP1/2, pUL37 and pUS3 [50]. HSV-1 also triggers cytoskeletal network rearrangement such as actin modification to facilitate the passage of viral particles through the PM. It is important to mention that these modifications are specific to entry mechanism employed by the virus [51-53]. Cellular factors are then hijacked by the virus to support the capsid trafficking toward the nucleus. In fact, the capsid circulates in the cytoplasm toward the minus end of microtubules (MT) by interacting with the motor protein dynein along with its cofactor dynactin [54]. This process is defined as being pH-independent. The second entry model is based on a phagocytosis-like mode of entry of the enveloped viral particles, following by the fusion of the viral envelope with the vesicular membrane in the cytoplasm [55]. In this process, the binding of gD to nectin-1 activates local actin rearrangement through the RhoA-GTPase activity, which promotes cellular protrusion

formation and viral particles uptake [47] . It was demonstrated that the interior of these vesicles was rich in nectin-1 and HVEM. Consequently, the low-pH inside those vesicles generated by the vacuolar H^+-ATPase induces the exposure of certain gB and gD domains which further promotes the interaction with their respective receptors and enables fusion [55-58] . As the first model, the capsid is then released in the cytoplasm and is translocated toward the nucleus by the same active transport. Alternatively, some groups suggested that HSV-1 release from these vesicles was pH-independent in C10 cells, which supports the idea that the virus uses different entry routes depending on the cell line [59]. Interestingly, Dr. Sodeik's laboratory demonstrated a pH-dependent mechanism in some cells as, in presence of a H^+-ATPase inhibitor, endocytosis of enveloped virus was driven by Na^+/H^+ exchanger (NHE) and p21 kinase activities [60]. Although HSV-1 employs cells specific entry processes, one observation that seems to be commonly accepted is that the formation of these vesicles does not occur through clathrin- or caveolin- derived endocytosis [48, 49, 59-61].

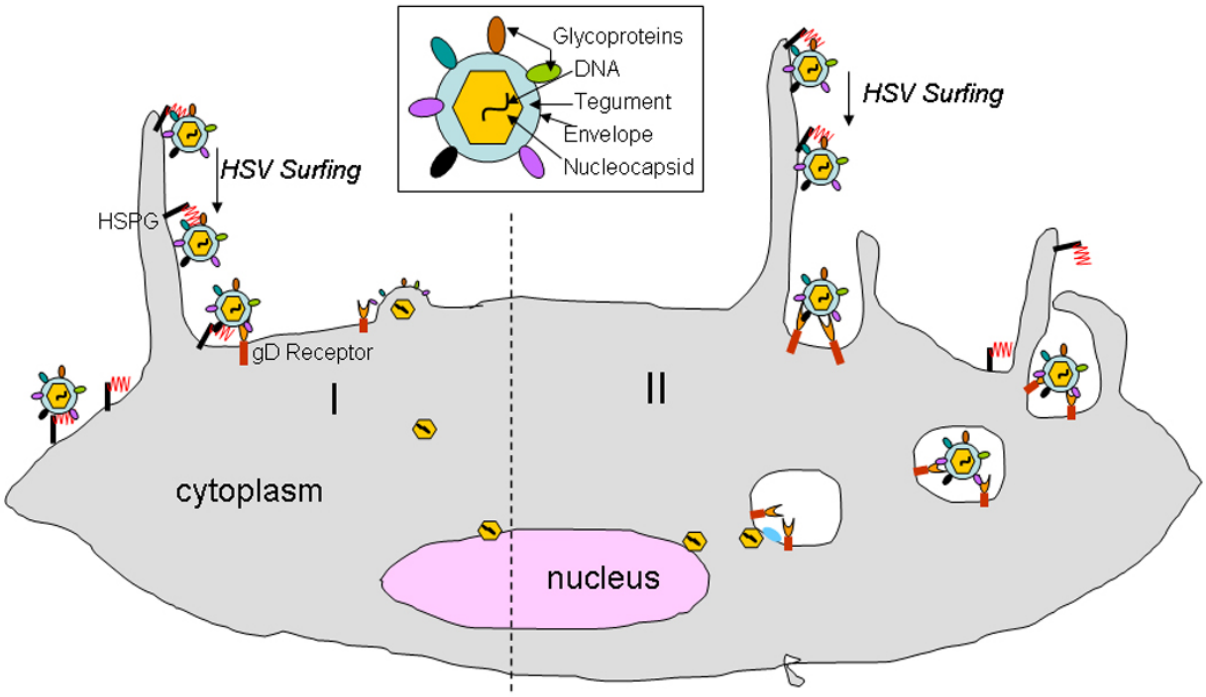

Fig 2. The two models of HSV-1 entry inside a cell

This figure is from a recent publication [62]. I: first entry mode where HSV-1 enters a cell through the fusion of its envelope with cellular PM. II: the second mode of entry is based on a

phagocytosis-like mechanism where the enveloped viral particles are uptaken in a vesicle, followed by the fusion of the viral envelope with the vesicular membrane in the cytoplasm.

1.3. Nuclear Entry

As other DNA viruses, HSV-1 replicates its viral genome inside the nucleus using its viral replicative machinery along with the cellular replicative machinery. To do so, HSV-1 must bypass the nuclear membrane (NM) barrier and inject its viral genome inside the nucleus. In fact, the mammalian NM is composed of two distinct membranes, the inner nuclear membrane (INM) and outer nuclear membrane (ONM), separated by the perinuclear space. This NM is impermeable to most molecules as it tightly regulates trafficking across the membrane using either passive diffusion of ions and molecules smaller than 10 nm or active transport of larger molecules, both through nuclear pore complex (NPC) [63, 64]. NPC is a transmembrane complex composed of 30 different proteins termed nucleoporins (Nup), organized into an octagonal funnel [65]. In its open conformation, the NPC core allows the passage of molecules up to 39 nm [66]. Consequently, when the 125 nm capsid reaches the nucleus, it interacts with NPC to subsequently release its genome inside the nucleus as the capsid cannot pass through the NM [67]. The capsid docking occurs through the binding of NPC cytoplasmic components Nup358 and Nup 214 and the minor capsid protein pU_L25 [50, 68]. It is not clear if the tegument protein VP1/2 also binds directly to NPC, but previous experiments demonstrated that antibodies against this tegument protein inhibit capsid docking [50]. Furthermore, studies also demonstrated that capsid docking was an importin-β and Ran GTPase dependent process [69, 70]. Following the docking stage, the release of the viral genome is initiated, a process that is thought to be energy independent [71]. Even if it remains unclear what triggers this process, a study demonstrated that VP1/2 hydrolysis is required, as its inhibition results in capsid docking with no DNA ejection [72]. The viral DNA exits the capsid through the portal vertex which is aligned with the NPC core. It was demonstrated that there was a high pressure inside the capsid due to the packaging of the large genomic DNA. Consequently, it is thought that this pressure is the driving force that allows the DNA to pass through the NPC [23, 73].

1.4. Viral Genomic Expression and Replication

To efficiently produce viral progenies, expression of the viral genes is sequentially regulated to ensure synthesis of viral components only when required. To depict this phenomenon, HSV-1 genes have been classified into three classes; the immediate-early genes (α) which are the first to be expressed, the delayed-early genes (β) and the late gene (γ) [74]. The γ class can be subdivided into the leaky-late (γ1) and true-late (γ2), where γ1 are expressed at a low level prior to DNA replication while γ2 are only expressed during viral DNA synthesis [75, 76]. α gene products are involved in β and γ gene expressions as they interact or recruit multiple cellular factors to support viral transcription. ICP0, ICP4, ICP22, ICP27, ICP47 are the viral proteins that are detected at early time points during the infection [77]. As for β gene products, they are mostly implicated in the viral genomic replication into a concatemeric DNA structure. γ genes are expressed at later time points during lytic replication as they required α and β gene products. Their expression results in the synthesis of proteins supporting capsid assembly, DNA encapsidation and nuclear egress [78, 79].

When the viral genomic DNA is inside the nucleus, it is suggested that it rapidly circularizes prior to any viral protein synthesis [17]. It was shown that the cellular DNA ligase was involved in DNA circularization [80]. Subsequently, cellular factors coordinate the assembly of viral DNA around nucleosome [81]. This process is thought to be part of the cellular defence mechanism as the nucleosome-associated-viral DNA is organized into a heterochromatin conformation which prevents gene expression [82]. To alleviate this silencing effect, a trimeric complex composed of two cellular and one viral proteins recruits cellular factors to modify nucleosomes, triggering a conformational switch from heterochromatin to euchromatin [83]. This complex is composed of the tegument protein VP16, which interacts with the host cell factor 1 (HCF1) in the cytoplasm [84]. HCF1 then mediates their translocation inside the nucleus where they associate with octamer-binding protein 1 (Oct1) [84]. This trimeric complex recruits histone modifiers such as LDS1, Set1 and MILL1 at the α gene promoters where the genome is now accessible to cellular transcription factors [85, 86]. Depending on the α gene promoter's unique response element composition, VP16 recruits the required cellular transcription factors along with the cellular RNA polymerase II to transcribe α genes.

As mentioned earlier, β gene expression results in the synthesis of the viral DNA replication machinery. To this day, there are seven essential proteins involved in DNA replication: ICP8 (U_L29), the single-stranded DNA binding protein; pU_L30 and pU_L42, each forming the catalytic and processivity subunits of the viral DNA polymerase respectively; pU_L9 which binds to one of the three replicative origins; and pU_L5, pU_L8 and pU_L52 that comprise the helicase/primase (H/P) complex [87, 88]. Following the synthesis of viral replication proteins, they merge together at what is termed the pre-replicative sites [89]. Those sites are located at the inner nuclear periphery where it is thought that input viral DNA accumulates upon nuclear entry. As DNA replication occurs, those sites, now defined as replicative compartments, grow and remain located at the nuclear periphery [90-92].

DNA replication starts at one of the three origins of replication; one located in the U_L sequence (oriL) and the other two located in inverted repeats of the U_S sequence (oriS). All three replicative origins are palindromic sequences flanked by AT-rich regions [93]. The oriL's AT-rich regions are flanked by two pairs of pU_L9 binding sites termed box I and box III [87]. The oriS' AT-rich regions are also flanked by pU_L9 binding sites, but box I and III are at the 5'end whereas a lower affinity pU_L9 box II is at the 3'end [87, 94]. Regardless at which origin pU_L9 binds, it interacts with ICP8 to destabilize the AT-rich region and initiate the opening of the viral dsDNA. When the replication fork is generated, the helicase/primase (H/P) complex is recruited to proceed to DNA unwinding and synthesis of DNA primers for the lagging strand [95]. As the ssDNA are formed from the H/P complex activity, ICP8 dissociates from pU_L9 to bind to the ssDNA, preventing re-annealing of complementary sequences [95, 96]. The viral DNA polymerase is then recruited to replicate the viral genome on both leading and lagging strands [75]. It was demonstrated that HSV-1 genome is replicated as head-to-tail concatemers through a rolling circle mechanism [17]. Some other studies suggested that DNA recombination might also play a role in the formation of the concatemeric genome [97]. Additionally to the major viral replicative proteins, some other viral proteins were identified as being implicated in DNA replication. Such viral proteins like thymidine kinase (U_L23), deoxypuridine triphosphatase (U_L50), ribonucleotide reductase (U_L39 and U_L40), uracil DNA-glycosylase (U_L2) and alkaline nuclease (U_L12) were all shown to be non-essential for viral replication but provide an advantage in non-dividing cells like neurons [87]. Several cellular factors associated

mostly with DNA repair mechanisms such as RPA, RAD51 or NBS1 are also involved in viral DNA replication as they are located at the replicative compartments [98-100].

1.5. Capsid Assembly and DNA Packaging

After capsid proteins have been translated in the cytoplasm, they are translocated inside the nucleus near replication compartments. There, VP5, VP26, VP23 and VP19C along with the scaffold proteins pU_L26 and $pU_L26.5$ assemble and form circular procapsids [101]. Procapsid angulation then occurs following conformational changes and scaffold protein maturation, where the proteolytic action of pU_L26 generates VP22a (from $pU_L26.5$), VP21 and VP24 (from pU_L26) [102, 103]. Angular capsids, now defined as capsids, are found in three subtypes in the infected nucleus: A, B and C. Following capsid assembly, newly synthesized viral genome must be cleaved into monomers [104]. Many γ gene products are implicated in those processes to ensure that only a single copy of viral DNA gets encapsidated to form competent viral progenies [105]. To this day, the mechanism underlying DNA cleavage is not clear, but some studies demonstrated that the viral genome is spliced and ligated at conserved sites termed *a* sequences [106]. This process is thought to occur during DNA packaging by a complex comprised of pU_L15, pU_L28 and pU_L33. DNA packaging is also mediated by pU_L6, pU_L17, pU_L25 and pU_L36 as they form the portal vertex (pU_L6) and the capsid vertex specific component (CVSC) (pU_L17, pU_L25 and pU_L36) respectively [104]. During DNA packaging, the viral genome gets inserted inside the capsid concomitant to some scaffold proteins displacement [104]. Studies of B capsids showed that their core is filled with VP22a along with some other scaffold proteins. Therefore, it is thought that B capsids are capsids that have not encountered DNA [104, 107]. As for A capsids, it was demonstrated that they are hollowed angular capsids, suggesting that DNA packaging might have started but failed during this process [108]. C capsids are the only type filled with the entire viral genome and eventually result in mature virions [109].

1.6. Nuclear Egress

After the viral DNA has been packaged inside the capsid, the filled capsid has to exit the nucleus. At this stage, the capsid must bypass the same barriers it encountered during nuclear entry but bring along both the viral DNA and capsid. To do so, capsids have to displace the

nuclear lamina and physically cross the INM and ONM. The most prominent model to describe nuclear egress is the envelopment/de-envelopment hypothesis. In this model, primary envelopment occurs through budding from the INM and was shown to be mediated by the heterodimeric complex pU_L31 and pU_L34 termed nuclear egress complex (NEC) [110, 111]. NECs are located at the luminal face of the INM and initiate capsid budding by interacting with many viral and cellular factors [112]. One important interaction during nuclear egress is recruitment of the viral kinase pU_S3 by NEC [111]. This kinase phosphorylates lamin A/C that is lining the luminal face of the INM [113]. NEC also recruits the cellular protein kinase C which phosphorylates lamin B [114]. Phosphorylation of lamin proteins promotes nuclear lamina's disassembly, along with marginal chromatins displacement which are tethered to it. This rearrangement of the nuclear architecture is thought to give the capsid a better access to the INM [110]. Following capsid docking, NEC interacts with tegument proteins ICP22 and pU_L47. Even if the exact function of those tegument proteins is yet to discover, mutations in ICP22 or pU_L47 result in reduced nuclear egress of capsids [115, 116].

NEC is the major component that triggers INM curvature and scission of the membrane to form a vesicle. When NEC is overexpressed without other proteins, it mediates vesicle formation at the INM [117, 118]. Therefore, it was suggested that other viral proteins might support capsid budding, but this process was performed mainly by the accumulation of NEC multimers at the site of membrane curvature [119]. As the nuclear membrane-derived vesicle is formed, NEC recruits the cellular endosomal sorting complex required for transport III (ESCRTIII) to scission the membrane and released the primary enveloped virion (PEV) into the perinuclear space [120].

In the envelopment/de-envelopment model, the second step of nuclear egress is the fusion of the PEV with the ONM to release the virion into the cytoplasm. Studies have demonstrated that the fusion machinery glycoproteins gB, gD, gH/L and the glycoprotein gM were found at the INM and associated with perinuclear virions [121, 122]. Additionally, the pU_S3 kinase is also implicated in the PEV-ONM fusion as it phosphorylates gB and pU_L31 [123, 124]. It is noteworthy that NEC is not implicated in this process. In fact, it dissociates from the PEV following pU_L31 phosphorylation resulting in its absence in cytoplasmic viral particles [125].

1.7. Tegumentation and Re-Envelopment

When the naked nucleocapsids get released in the cytoplasm, tegumentation and re-envelopment must be performed to produce infectious particles. The molecular details describing those processes are yet to be elucidated, but some works suggested that tegumentation occurs through protein-protein interactions [29, 126]. Furthermore, it seems that teguments are incorporated in a sequential manner as some of them remained associated with naked cytoplasmic capsids following nuclear egress while others are added later on during viral egress. It was demonstrated by our laboratory and other groups that U_S3, U_L36, U_L37, ICP0 and ICP4 are incorporated onto nuclear capsids before their release into the cytoplasm [111, 127-129]. However, much evidence hints that the majority of tegument proteins are incorporated at the TGN as newly synthesized viral particles were shown to co-localize with TGN markers [26, 29]. Since the Golgi apparatus is the organelle where final post-translational modifications occur, it is not surprising that mature viral proteins are incorporated at this site. The re-envelopment model also suggests that the outer membrane of mature virions is decorated with viral glycoproteins acquired at this site [28]. Although re-envelopment is not precisely understood, some viral factors were shown to promote it. Hence, it was demonstrated that the viral glycoproteins gE/I and gD were involved in re-envelopment as deletion of those glycoproteins generate accumulation of unenveloped capsids in the cytoplasm [130]. Moreover, it was observed that L particles (vesicles containing tegument proteins and glycoproteins, but no capsid or viral genome) undergo secondary envelopment using the same pathway as viral particles [131]. Those data give strong evidence that re-envelopment can be mediated by teguments and glycoproteins regardless of the presence of the capsid [132, 133]. Enveloped nucleocapsids finally leave the TGN by budding out into vesicles. This process was shown to be regulated by the cellular protein kinase D (PKD), as its downregulation results in a lower extracellular viral yield and capsid accumulation at the TGN [134]. Those vesicles containing nucleocapsids are targeted to the plasma membrane by hijacking the cellular secretory pathway for their own transport [135, 136]. They eventually fused with the plasma membrane and release mature virions in the extracellular space where the virus can infect neighbouring cells.

1.8. Cell-to-Cell Spread

Although HSV-1 can infect neighbouring cells by releasing newly synthesized viral particles into the extracellular space, cell-to-cell spreading was demonstrated to be employed by the virus. Indeed, virion containing vesicles fused at the cell's periphery PM where tight junctions between neighbouring cells are found. The virus then enters and propagates as previously described in nearby cells [137]. This infection method provides an evolutionary advantage as it allows the virus to expand its infection without being neutralized by antiviral antibodies produced by the host. It is also an essential mechanism to establish latency as viral particles travel from mucosal epithelium to trigeminal ganglions (TG) using this process [138, 139]. During reactivation, HSV-1 then employs the same mechanism to reach back the epithelium cell layer [140].

It was determined that the gE/gI complex was an important factor to mediate cell-to-cell infection [141]. In animal model experiments, viruses lacking this complex did not reach neurons and failed to establish latency. Additionally, ΔgE/gI viruses produced smaller plaques than their wild type counterpart when titrated on a cell monolayer [139, 142, 143]. A heterotrimeric complex comprised of the pU_L16, pU_L21 and pU_L11 was shown to interact with the gE cytoplasmic tail and influence the cell-to-cell mechanism of the virus [144]. gK was also demonstrated to promote cell-to-cell spreading in culture and animal experiments [145]. Interestingly, in *in vitro* experiments using BHK and Vero cells, gK and the membrane protein U_L20 have an anti-fusogenic activity when overexpressed with the core fusion machinery gB,gH/gL and gD. In those studies, formation of syncytia (multinucleated cell) increased when cells were infected with mutated-gK viruses, suggesting that gK-U_L20 prevents viral-mediated aberrant cell fusion between surrounding cells [146].

1.9. gM and E-Syt 1 Interaction

As illustrated earlier, proper HSV-1 trafficking requires multiple steps of fusion between various cellular compartments. While some viral proteins promote fusion, others inhibit this process, which demonstrates that HSV-1 can tightly modulate its own fusogenic machinery. As substantially described in the literature, gM is a transmembrane protein found in many cellular compartments during infection [35]. Indeed, early during infection, it is detected at the NM

while it is detected at the TGN and cellular surface at later times [35, 147]. Although it is defined as a non-essential glycoprotein in culture, gM was shown to interact with the viral fusion machinery as it participates in the translocation of gD and gH/gL to viral assembly site during viral egress [148-150]. Furthermore, mutated gM seems to reduce viral infectivity and promote accumulation of unenveloped nucleocapsid in the cytoplasm [147, 151]. Some other groups also demonstrated that ΔgM-virus generated a lower viral titer *in vivo*, and that the same virus could not efficiently spread throughout the nervous system [152]. Although protein interactions among viral proteins were substantially elucidated [29], it remains unclear for many processes which cellular protein are hijacked by the virus and how those interactions contribute in efficient viral production. For such purpose, previous experiments in our laboratory tried to unveil cellular proteins interactions with gM, a mediator of viral fusion machinery. Mass spectrometry (MS) and co-immunoprecipitation (co-IP) data demonstrated that not only gM interacts with the viral glycoprotein gN, but also with the cellular protein Extended-Synaptotagmin1 (E-Syt1) [35, 153]. In fact, when the lysate from infected cells were subject to anti-E-Syt1 or anti-gM in co-IP experiments, both proteins were reciprocally detected. Likewise, when cells were only transfected with those two proteins, they co-precipitated together which suggest that their interaction is independent of other viral proteins [153]. Interestingly, published data from our laboratory demonstrated that downregulation of E-Syt1 using small interfering RNA (siRNA) significantly increases the viral titer in the supernatant [153]. In agreement with those data, E-Syt1 knockdown cells had more viral particles at their cell surface (53%) compared to the mock treated cells (30%). Similarly, viral entry was also elevated when E-Syt1 was downregulated [153]. Moreover, increasing numbers of syncytium were observed when E-Syt1 and the related E-Syt3 were both knocked down, again reinforcing the importance of this cellular protein in fusion mechanisms and proper viral propagation [153]. Altogether, E-Syt1 seems to have an inhibitory effect on viral production as lower levels of this protein promotes HSV-1 propagation.

1.9.1. E-Syt1

As for HSV-1, cellular trafficking and signalling are tightly regulated by the fusion machinery. Indeed, there is a large variety of proteins that play a role in coordinating those important cellular processes in order to maintain cell homeostasis. One important fusogenic family is the SNAREs where 36 different members are found in mammalian cells [154, 155].

They can be subdivided into 2 groups which comprise vesicle (v or R)-SNAREs located on circulating vesicle membranes and targets (t or Q)-SNAREs located on the targeted fusion sites [156]. As example, VAMPs/synaptobrevins and Synaptotagmins are members of R-SNAREs whereas SNAP-25 and syntaxin 1 are members of Q-SNAREs, all found in mammalian cells [157-159]. One SNARE paralog are the mammalian extended-synaptotagmin (E-Syt) proteins [160]. Their name originates from sequence homologies with the SNARE protein synaptotagmin (Syt). Where Syts only have two C2 domains, the "extended" version, E-Syts, can have three to five C2 domains [161]. Despite their sequence similarities, their functions and localization varies. Human synaptotagmin 1 (Syt1) is found at neuronal axon terminals where they regulate exocytosis of neurotransmitters from vesicles [162, 163]. In contrast, human E-Syts are located at the endoplasmic reticulum-plasma membrane (ER-PM) junction where they induce the tethering of those two membranes without initiating fusion. C2-containing proteins are also found in other organisms like yeast. While yeasts don't express Syts, they express an ortholog version of E-Syts, tricalbins (Tcb), which perform similar functions [161, 164].

1.9.2. E-Syt1 Structure

As mentioned earlier, E-Syts are transmembrane tethering proteins that allow two membranes to significantly reduce their distance. In humans, this family subdivides into three different isoforms referred as E-Syt1, E-Syt2 and E-Syt3.

E-Syt1 is 1114 amino acids long and is anchored at the endoplasmic reticulum (ER) through an N-terminal hairpin like structure. This hairpin structure has a 30 hydrophobic amino acids stretch which enables the protein to interact with the phospholipids found at the ER membrane. Due to this hairpin conformation, the N- and C-terminal of E-Syt1 are both oriented toward the cytosolic portion of the cell. Following the hydrophobic stretch, there is a synaptotagmin-like mitochondrial lipid-binding proteins (SMP) domain that has a β-barrel conformation. It was demonstrated that this SMP domain is involved in the dimerization (homodimers of E-Syt1/1 or heterodimers of E-Syt1, 2 or 3) of the different isoforms [165]. Additionally, many studies suggest that SMPs are also implicated in the shutting of multiple types of phospholipids between two membranes through their highly hydrophobic core [166-168].

Downstream of the SMP sequence, there is five C2 domains named C2A, C2B, C2C, C2D and C2E which enable E-Syt1 to perform its functions as a calcium sensor and lipid interactor [55, 160]. The C2C domain functions as the calcium binding subunit where it interacts with the calcium present in the cytosol [169]. As a result of calcium binding, conformational changes in E-Syt1 induces the formation of homodimers which are then translocated to the ER-PM junction [169]. At this site, the C2E domain functions as the lipid binding subunit where it directly binds to phosphatidylinositol-4,5-bisphosphate ($PI(4,5)P_2$) found at the PM [168, 169]. To this day, it is unclear what are the exact functions of C2A, C2B and C2D domains. One group suggested that C2A can also bind to Ca^{2+}, which alleviates its inhibitory effect on the SMP domain to allow the transfer of glycerophospholipids [170].

E-Syt 2 and 3 have a similar structure as E-Syt1. They diverge in their number of C2 domains, where E-Syt 2 and 3 only have three named C2A, C2B and C2C. Nonetheless, their C2 domains performed the same functions as the ones from E-Syt1. In E-Syt2 and 3, C2A is the calcium sensor while C2C binds to the $PI(4,5)P_2$ at the PM [161].

At rest, there are less than 1% of the PM areas where ER-PM junctions are maintained constitutively by E-Syt2/3 at about 20 nm [171, 172]. Those ER portions are referred to as cortical ER. When the cytosolic Ca^{2+} concentration increases and E-Syt1 gets translocated to those areas, the cortical ER expands, which increases the ER-PM junction's surface area and the distance between the two lipid bilayers can get as close as 10 nm [173].

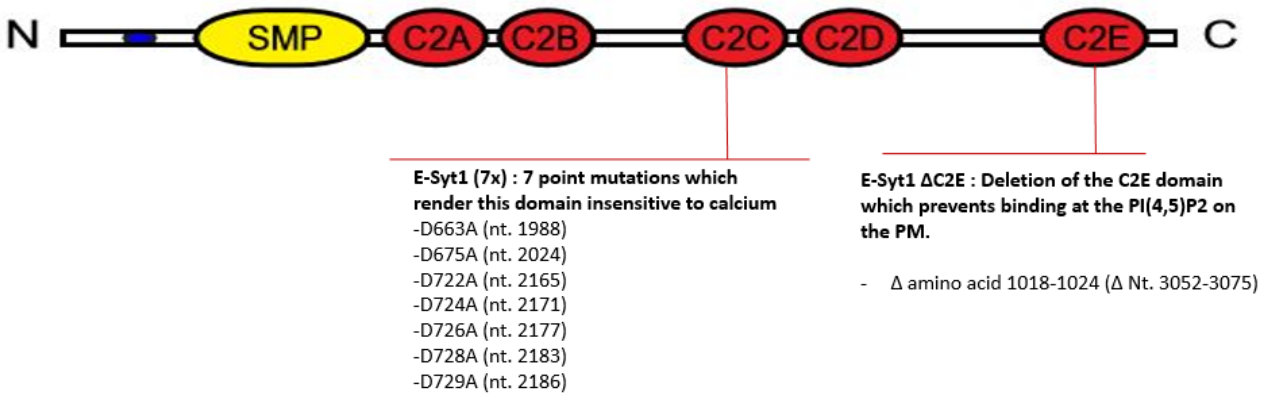

Fig 3. Structure of E-Syt1 and mutations used in this study

The illustration was modified from a recent publication [160]. The figure illustrates the different domains of wild type E-Syt1. The specific mutations used to abrogate the function of E-Syt1 are also illustrated.

1.9.3. E-Syt1 Activation

Calcium is a molecule involved in many cellular processes such as membrane depolarization, signalling pathways or apoptosis [174-176]. Consequently, calcium mobilization is tightly regulated, preventing activation of unnecessary pathways. In mammalian cells, the ER, mitochondria and Golgi apparatus are the compartments where calcium is stored, with ER being the predominant one [177-179]. In order to recruit E-Syt1 at the ER-PM junction, there must be a significant change in the cytoplasmic level of Ca^{2+}. At rest, the cytosolic Ca^{2+} concentration range from 50 to 100 nM [180]. This low calcium level is tightly maintained by the activity of the sarco/endoplasmic reticulum Ca^{2+} ATPase (SERCA) and the plasma membrane Ca^{2+} ATPase (PMCA) [180, 181]. At that state, E-Syt1 is dispersed randomly throughout the ER [161]. Upon an external stimulus via various signaling molecules, phospholipase C (PLC) gets recruited and activated through the activity of G proteins or tyrosine kinase pathways [182-184]. Activated PLC hydrolyzes $PI(4,5)P_2$ from the PM, generating soluble inositol triphosphate (IP_3) and diacylglycerol (DAG). Soluble IP_3 binds to the IP_3-receptor (IP_3-R) found at the ER membrane outer leaflet, which triggers the release of ER-Ca^{2+} storage in the cytosol. The change of ER-Ca^{2+} concentration is rapidly detected by the ER-Ca^{2+} refilling mechanism that induces the translocation of STIM1 at the ER-PM junction. There, STIM1 interacts with Orai1, found at the PM, to actively pump calcium inside the cytosol from the extracellular environment. The large influx of extracellular Ca^{2+} induces a sustained and significant increase in the cytosolic Ca^{2+} concentration in the millimolar range which triggers the translocation of E-Syt1 at the ER-PM junction. This large calcium influx not only induces the ER-PM junction expansion, but also supports other cellular processes that require Ca^{2+} signalling, metabolism and membrane depolarization. The calcium concentration is then actively brought back to resting level through SERCA activity that replenishes the ER-Ca^{2+} storage and PMCA that pumps Ca^{2+} outside the cell. This process of extracellular calcium influx is referred as store-operated Ca^{2+} entry (SOCE) which is independent of E-Syt1 translocation, but is required for E-Syt1 recruitment [170, 172, 173, 185].

1.10. Calcium and HSV-1

Since calcium was demonstrated to participate in cellular trafficking and cytoskeletal rearrangement [186-188], it is not surprising that HSV-1 hijacks this process to its advantage. Indeed, it was observed that intracellular calcium increases upon HSV-1 entry [188]. When calcium elevation was blocked by pharmaceutical drugs targeting ER-Ca^{2+} release, viral entry diminished significantly [189]. One group even concluded that calcium release is mediated by the interaction between the viral fusogenic machinery and the cellular receptors syndecan-2, nectin-1 and integrin αV [190]. Whilst many studies provided evidence of calcium implication during viral entry, it remains unknown if calcium is required during egress, and if so, at which stage.

1.11. Hypothesis and Approach

Given previous data from our laboratory suggesting the inhibitory effect of E-Syt1 on viral propagation, the main objective of this project was to test the hypothesis that E-Syt1 negatively modulates HSV-1 egress by limiting the trafficking of newly synthesized viral particles toward the PM. We further hypothesize that this regulatory function is linked to E-Syt1's capacity at sensing calcium and interacting with $PI(4,5)P_2$.

To investigate the regulatory effect of E-Syt1 on HSV-1, full-length E-Syt1 along with calcium sensing and lipid binding deficient mutants were overexpressed in HSV-1 permissive cells. The viral titer was then measured to evaluate the effect of those proteins on viral egress. In parallel, the implication of calcium on HSV-1 egress was also evaluated using two different calcium chelators, EGTA and Bapta-AM, as well as the calcium-release inducer ionomycin. Those drugs were added at different time points during the infection to evaluate at which moment calcium was required. Likewise, viral titers were measured to determine the effect on viral egress.

2. Material and Methods

2.1. Cell line

Hela (cervical adenocarcinoma) and Vero (African green monkey) cells were obtained from the American Type Culture Collection (ATCC). They were cultured in 1x Dulbecco's Modified Eagle Medium containing 5% bovine growth serum (BGS) and 1% L-Glutamine. Cells were cultured at 37°C with 5% CO_2 and passaged when 90% confluent. They were also regularly tested for any mycoplasma contamination, which was absent. In all experiments, HeLa cells were used to produce the virus in different conditions (see below) while the Vero cells were employed to titer viral yields under those conditions.

2.2. Viruses and Infection

All virus stocks were produced on Vero cells and harvested 48-72 hours post-infection (hpi). The viral titer of the supernatant and cell lysate were subsequently measured by plaque assay.

2.2.1. HSV-1 17+ WT

This virus was obtained from the laboratory of Dr. Sodeik[1]. It is a 17+ strain which has the wild type viral genome. Prior to the infection, Hela cells were seeded in the appropriate dish for 24 hours at 37°C with 5% CO_2. The day of the infection, cells were suspended in culture medium and counted to determine the proper amount of virus corresponding to a multiplicity of infection (MOI) of 5. The viral stock was diluted in Roswell Park Memorial Institute (RPMI) media containing 0.1% bovine serum albumin (BSA) and then added to the cell monolayer. After 1 hour of absorption at 37°C and 5% CO_2, complete 1x DMEM was added to the infected cells. Eighteen to twenty-four hpi, the supernatant and the cell lysate were harvested for subsequent analysis. Briefly, the supernatant was simply harvested by collecting the media. Subsequently, the cell lysate was harvested by scraping the monolayer of infected cells in 1x phosphate-buffered saline (PBS) containing a cocktail of protease inhibitors (CLAAAP).

[1] Institute of Virology, Hannover Medical School, Carl-Neuberg-Str. 1, Hannover, D-30625, Germany.

Following a centrifugation at 500x g for 10 min at 4°C, the supernatant was removed and fresh 1x PBS containing CLAAAP was added to pellet. The pellet was then re-suspended and subjected to 3 cycles of freeze-thaw in liquid nitrogen and 37°C water bath. Both fractions were stored at -80°C for subsequent analysis.

2.2.2. HSV-1 V701

This virus was obtained from Dr. Register[2]. This 17+ strain virus has 2 point mutations in the U_L26 protease gene [191]. Those mutations render the virus thermosensitive, which inhibits the egress of newly synthesized viral particles at 39°C but allows it at 31°C. As previously mentioned, Hela cells are seeded 24 hours prior infection. Using a MOI of 2 for the infection, complete 1x DMEM at 39°C was added after 1 hour of absorption. The infected cells were incubated at 39°C for 4 hours and then incubated at 31°C for 14 hours. Eighteen hpi, the supernatant and the cell lysate were harvested for subsequent analysis as describe previously.

2.2.3. HSV-1 K26 GFP

This virus was obtained from the laboratory of Dr. Desai[3]. It is derived from the KOS strain and has a green fluorescent protein (GFP) fused with the viral protein VP26. VP26 is an accessory component of capsids [192]. It is a late protein which allows the observation of circulating mature capsids inside the cell. As previously mentioned, Hela cells were seeded 24 hrs prior infection in complete 1x DMEM at 37°C on coverslip. Cells were then infected with a MOI of 5 and mounted in Hoechst-Dako 18-24 hpi. The localization of the virus inside the cells were monitored using the fluorescent Zeiss axio-imager Z2 microscope and analyzed with ZenPro software.

---

[2] Department of Biological Chemistry, Merck Research Laboratories, West Point, PA 19486, USA.

[3] Department of Pharmacology and Molecular Sciences, Johns Hopkins University School of Medicine, Baltimore, Maryland 21205, USA.

2.3. Plasmids

All the plasmids were produced by transformed *E.Coli* DH5α strain and isolated with NucleoBond Xtra midi kits (Macherey-Nagel). To confirm that there was no undesirable mutation in the gene of interest, all plasmids were sequenced.

2.3.1. EGFP E-Syt1 WT, mCherry E-Syt1 (7x) and EGFP E-Syt1 ΔC2E constructs

Those plasmids were obtained from Dr. De Camilli[4] [193]. The expression of E-Syt1 was confirmed by immunofluorescence and western blot.

The first plasmid, EGFP E-Syt1WT, contains the WT version of E-Syt1 tagged with a GFP protein at its N-terminus. This modification does not affect the proper folding or the ER localization of E-Syt1 in the cell [193].

The second plasmid, mCherry E-Syt1 (7x), contains E-Syt1 tagged with mCherry at its N-terminus, which also doesn't affect the proper folding or the ER localization of E-Syt1 in the cell [193]. This protein has seven point mutations in its C2C domain which abolish its calcium sensing function (figure 3). The seven point mutations in the C2C domains result in amino acid substitutions from aspartic acid to alanine. Upon sequencing, we identified an expected stop codon at nucleotide 3334. A site-directed mutagenesis was performed to eliminate this nonsense mutation. Briefly, the site-directed mutagenesis was performed using the QuikChange II XL Lightning site-directed mutagenesis kit (Agilent) and the primers illustrated in table 1. The qPCR experiment was performed using the following program in a Biometra Thermocycler T-Gradient Thermoblock:

- Initial denaturation: 1 cycle: 95°C, 1 min
- Amplification: 18 cycles: 95°C, 50 sec / 50°C, 50 sec / 73°C, 8.033 min
- Final extension: 1 cycle: 68°C, 1 min

[4] Department of Cell Biology, Program in Cellular Neuroscience, Neurodegeneration, and Repair, and Howard Hughes Medical Institute, Yale School of Medicine, New Haven, CT 06510, USA.

Fifty nanograms of the modified mCherry E-Syt1 (7x) construct was transformed into XL10-Gold ultracompetent bacteria and the antibiotic kanamycin was used at a concentration of 50 µg/ml as the selective agent. The plasmid was extracted following the DNA extraction kit protocol (Qiagen) and a second sequencing analysis validated that there was no other unexpected mutation in the sequence.

Table 1. Primer sequences used to remove the stop codon in mCherry E-Syt1 (7x) protein

nucleotide	strand	Primer sequence
T3334C	Sense	tccatgtattagaggccCaggacctgattgccaaa
T3334C	AntiSense	tttggcaatcaggtcctGggcctctaatacatgga

The third plasmid, EGFP E-Syt1 ΔC2E, contains the E-Syt 1 protein tagged with a GFP at its N-terminus. This protein has a deletion of 441 nucleotides (from nucleotides 2871 to 3313) resulting in the absence of the C2E domain. A sequencing experiment validated the absence of this domain, and no other mutation was found in the sequence.

2.3.2. EGFP-N2

This plasmid was obtained from Invitrogen and was used as a DNA control for the transfected-infected cells. The expression of the GFP protein was confirmed by immunofluorescence and western blot.

2.3.3. pCyto-gBFull

This plasmid was obtained from Dr. Desjardin[5]'s laboratory. This plasmid was used to create the standard curve in qPCR experiments to quantify viral genome copies as it contains the full sequence of gB.

[5] Department of Pathology and Cellular Biology, University of Montreal, C.P. 6128, Succ. Down-Town, Montreal, QC, H3C 3J7, Canada.

2.4. Transfection

The transfection agent used in those experiments was Lipofectamine 3000. Twenty-four hours prior to the transfection, Hela cells were seeded in 24- or 6-well plates to obtain a 60-70% confluence. As described in the manufacturer's protocol, the appropriate amount of DNA and lipofectamine 3000 were diluted in Opti-MEM. The DNA-Lipofectamine complex was added to the culture media containing Hela cells. Depending on the experiment, the transfected cells were either used in subsequent manipulations or mounted in Dako-Hoechst for immunofluorescent analyses 12-24 hours post transfection.

2.5. Plaque Assay

Viral titers in the supernatant and cell lysate were determined by plaque assays. Twenty-four hours prior the titration, Vero cells were seeded in 6-well plates to obtain a confluent monolayer of cells. Samples containing an unknown amount of viruses were diluted in the appropriate amount of RPMI-0.1% BSA and added to the monolayer of Vero cells. For the supernatant, samples were diluted from 1,000 to 100,000 times the original concentration whereas the cell lysate fractions were diluted from 1,000,000 to 100,000,000 times. One hour after the absorption, 2x complete DMEM mixed with 2% agarose in a 1:1 ratio was added to the infected monolayer. Depending on the virus present in the sample, the infected cells were incubated at 37°C (HSV-1 17+ WT) or 31°C (HSV-1 V701). Three days post-infection (dpi) for the wild-type virus or 5 dpi for the V701 virus, the DMEM-agarose media was removed from the monolayer and the cells were fixed using -20°C cold 100% methanol. A solution of 0.1% crystal violet was subsequently added to the fixed cells to stain them. By taking into account the dilution and the volume plated, the initial viral titer was calculated using the number of plaque forming unit produced by the virus in each sample. The following equation was used to calculate the viral titer in each sample:

$$\text{Viral titer (pfu/ml)} = (\#\text{plaques} / \text{volume plated (ml)}) \times \text{dilution}$$

2.6. Western Blot

E-Syt1 expression was monitored by western blot. Thirty micrograms of proteins from the cell lysate of each sample was mixed with 1x sample buffer and 0.1% β-mercaptoethanol. They were then heated at 95°C for 10 min and run on an 8% SDS-PAGE gel at 130 V. The proteins were subsequently transferred on a PVDF membrane (Bio-Rad) and blocked for an hour in a 5% milk/ 1x PBS/ 0.1% Tween20 (Sigma) solution. The primary antibody, anti-E-Syt1 (Bethyl laboratory, 1:1000), Anti-GFP (Roche, 1:1000) or anti-Gamma tubulin (Sigma, 1:10 000), was added to the membrane for an overnight incubation at 4°C. The membrane was then washed three times with a 1X PBS/0.1%Tween20 solution, and incubated with the second antibody, Goat-anti-Mouse (Jackson ImmunoResearch, 1:10 000) or Goat-anti-Rabbit (Bethyl laboratory, 1: 10 000) conjugated with horseradish peroxidase (HRP) enzyme, for 1 hour at room temperature. Proteins on the membrane were revealed using the ChemiDoc XRS+ system (Bio-Rad) after the addition of ECL substrate (Bio-Rad).

2.7. Drugs

Bapta-AM (Abcam) was diluted in sterile DMSO and was used at a final concentration of 10 µM and 20 µM. EGTA (Sigma) was diluted in sterile water and was used at a final concentration of 0.5 mM. Ionomycin (Sigma) was also diluted in DMSO and used at a concentration of 2 µM. Both chelators and ionomycin were directly added to the culture media at 4, 6, 12 and 16 hpi.

Phosphonoacetic acid (PAA) (Sigma) was diluted in sterile water and used at a final concentration of 0.2 µg/ml. It was directly added to the media containing Hela cells and washed off by changing media at the required time.

2.8. Immunofluorescence

Cells seeded on coverslip were fixed with a 3% paraformaldehyde (PFA) solution and permeabilized with 0.1% triton. Thereafter, they were incubated at room temperature for 30 minutes in a blocking solution of 10% fetal bovine serum (FBS). Diluted in the same blocking solution, the primary antibody, Anti-VP5 (East Coast Bio, 1:100) or Anti-Calnexin (Thermo

Fisher, 1:50) were added to the cells for 1 hour. After three washes with 1x PBS, the secondary antibody, goat-anti-mouse Alexa 488 (Molecular Probes, 1:1000) or chicken-anti-mouse Alexa 568 (Molecular Probes, 1:1000), was added to the cells for 45 minutes. Coverslips were mounted in Hoechst-Dako on a microscope slide, and images of the cells were captured with a Zeiss axio-imager Z2 epifluorescence microscope and analyzed with ZenPro software.

2.9. qPCR

Quantification of the viral genomic DNA in the supernatant and cell lysate was performed by quantitative Polymerase Chain Reaction (qPCR) using the Perfecta Sybr Green supermix kit (Quanta bioscience 95054-500). The gene targeted for this experiment was gB. Briefly, viral genomic DNA was extracted from each sample using the GenElute mammalian genomic DNA miniprep kit and protocol without the use of DNAse (Sigma). Following the manufacturer's protocol, the appropriate amount of Sybr Green was mixed with the extracted DNA and the primers to amplify a portion of the gB gene. To convert the Cq value into DNA copy numbers, a standard curve was also performed using a known amount of a plasmid (pCyto-gBFull) containing the sequence of gB. The qPCR experiment was performed using the following program in Light Cycler 480:

- Preincubation : 1 cycle: 95°C, 5 min
- Amplification: 45 cycles : 95°C, 5 sec / 56°C, 10 sec / 72°C, 10 sec
- Melting curve : 1 cycle: 95°C, 1 sec / 65°C,1 min

2.9.1. Infectivity ratio

To calculate the infectivity ratio, the total pfu was divided by the number of total genome copies. Each treatment was normalized to the untreated condition as it represents the wild type infectivity. Values under or over 100% would imply that the resulting viral particles are less or more infectious than in the untreated condition.

2.10. Viability test

2.10.1. Drugs

Hela cells were seeded in a 96-well Greiner black plate 24 hours prior the viability test. Cells were then treated with one of the following drugs: 0.5 mM EGTA, 10 µM or 20 µM Bapta-AM or 2 µM ionomycin. Alamar blue (Bio-Rad) was added to each condition 12 hours post-treatment and the fluorescence was measured 18 hours post-treatment. As a control, the viability of untreated cells was also measured.

2.10.2. Transfection

Hela cells were seeded in a 96-well Greiner black plate 24 hours prior the viability test. Cells were then transfected as described previously in the section 2.4. Alamar blue was added 19 hours post-transfection and the fluorescence was measured 24 hours post-transfection. As a control, the viability of untreated cells was measured.

2.11. Statistics

Multiple comparisons ANOVA using the Dunnett's test was performed to determine all statistical significance of our data. Briefly, each mean value was compared to the control condition and the probability (*p*) value was calculated by the software Prism8 from GraphPad. Difference between the control and the experimental condition was considered statistically significant when *p* value was smaller or equal to 0.05.

3. Results

3.1. Calcium is required for HSV-1 egress

As mentioned previously, efficient viral entry is associated with transient calcium elevation inside the cells. To determine if calcium was also required during viral egress, Hela cells were infected with HSV-1 17+ WT virus at a MOI of 5 then subjected to the calcium chelator Bapta-AM (10 µM and 20 µM) or EGTA (0.5 mM) at 6 hpi. This time was selected to avoid measuring calcium impacts during the entry phase. Both chelators are very similar as they reversibly bind free calcium, but the acetoxymethyl (AM) ester derivative renders Bapta-AM cell-permeable. In fact, AM ester groups bind and neutralize the aminopolycarboxylic acid moieties of Bapta, which enable it to passively cross the PM [194, 195]. In the cytoplasm, the AM ester group is hydrolysed by cellular esterase, which enables the chelator to bind to two calcium molecules and prevent it from crossing the PM again [196]. Hence, EGTA chelates exclusively extracellular calcium in the media whereas Bapta-AM chelates cytosolic calcium. Those two calcium chelators were used at concentrations that were previously shown to significantly decrease the calcium concentration in the cytosol or the supernatant [197, 198]. Furthermore, a viability assay using Alamar blue was performed to ensure that those drug concentrations were not cytotoxic for Hela cells (figure 4). At 18hpi (i.e. 12 hours in the presence of drugs), the supernatant was harvested as described in the method section and viral titers were determined by titrating each sample on a monolayer of Vero cells. Data from figure 5 demonstrate that the presence of Bapta-AM reduced significantly the viral load in the supernatant whereas EGTA did not have much effect compared to mock-treated infected cells. Additionally, the effect of Bapta-AM was concentration dependent as the decrease of the viral load was greater with a higher concentration of Bapta-AM. Next, the location of viral particles was compared between each treatment by immunofluorescence (IF) to determine if those drugs affected the trafficking of newly synthesized viruses inside the cell. To observe *de novo* viral particles, an antibody against the capsid protein VP5 was employed. VP5 is detected at the nucleus at early stages during the infection as it is the site of capsid assembly [199]. During viral egress, VP5 is also detected in the cytoplasm as the newly synthesized viral particles circulate toward the PM [200,

201]. Thus, the immunodetection of VP5 concurs with the detection of viral particles as VP5 is not found as free protein in the cytoplasm. From figure 6, we can see that the viral localization was similar among each condition. Taken together, the data indicates that sequestering intracellular calcium affects viral egress without disturbing the localization of viral particles inside the cell.

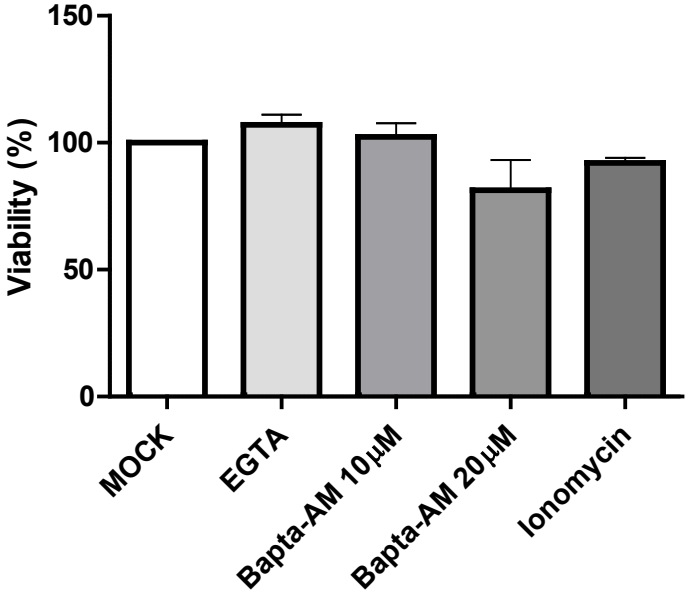

Fig 4. Hela cell viability is not affected by the different calcium chelators or ionomycin treatments

Hela cells were treated with 0.5 mM EGTA, 10 or 20 µM Bapta-AM or 2 µM ionomycin, as mentioned in the results section. Untreated cells (mock) were used to normalize the data (100%). Twelve hours post-treatment, Alamar blue was added to each condition and fluorescence was measured at 18 hours post-treatment. Each measurement was performed in triplicate and the average of three independent experiments is represented. Error bars represent the SEM and statistical analysis was performed by one-way ANOVA. No statistically significant differences were noted.

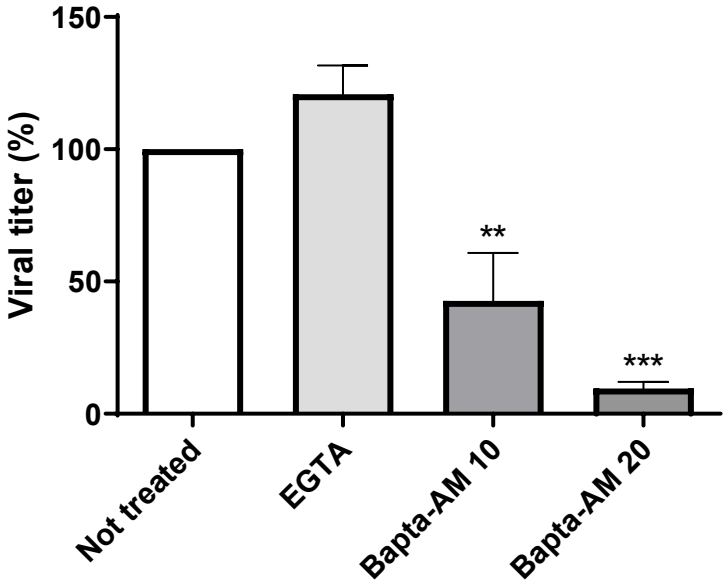

Fig 5. Chelation of intracellular calcium inhibits viral egress

Hela cells were infected for 18 hours at a MOI of 5 with HSV-1 17+ WT virus. Drugs were added at 6 hpi and the supernatant of each condition was harvested at 18 hpi. Viral titers were measured by plaque assay (see Materials and Methods). EGTA= 0.5 mM, Bapta-AM= 10 or 20μM. n=3, error bars represent the SEM, statistical analysis by one-way ANOVA where *p* values are ≤ 0.05;*, ≤ 0.01; ** and ≤ 0.001; ***.

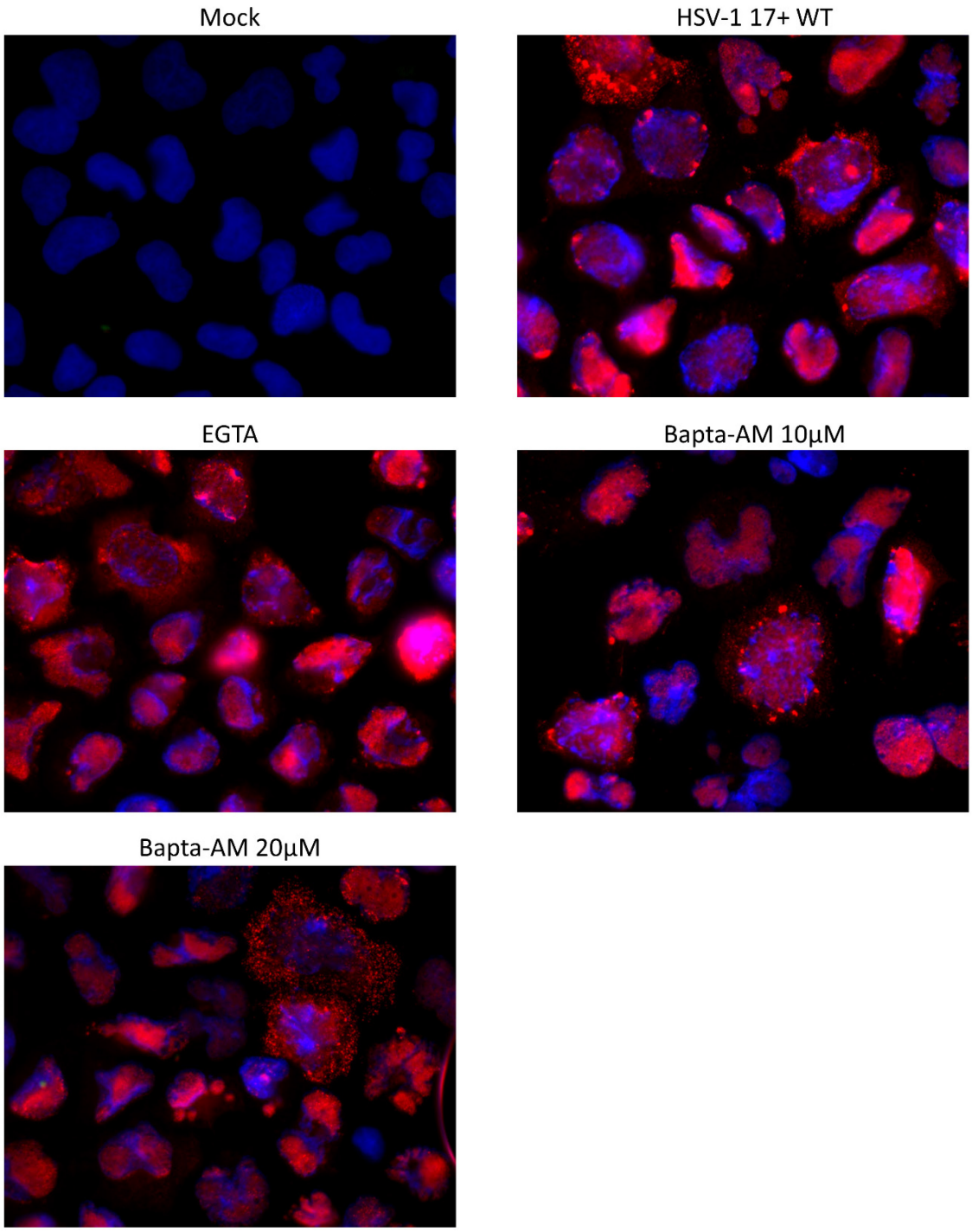

Fig 6. Viral localization inside the cell is not affected by post entry calcium level changes

Hela cells were infected for 18 hours at a MOI of 5 with HSV-1 17+ WT virus. Drugs were added at 6 hpi and infected cells were fixed and permeabilized at 18hpi. Viral particles were detected using the

primary antibody Anti-VP5 and a goat-anti-mouse Alexa 568 secondary antibody. Images are representative of three independent experiments (n=3).

3.2. Calcium Is Required at Early Time Points During HSV-1 Egress

To more specifically monitor the impact of calcium on viral egress, Hela cells were infected with the thermosensitive HSV-1 (HSV-1 V701) to synchronize the infection. This virus carries a mutation at the pU_L26 protease which inhibits nuclear egress of newly synthesized capsid at 39°C, but allows it at 31°C [191]. To synchronize the release of viral particles, infected Hela cells were incubated at 39°C for 4 hours then incubated at 31°C for an additional 14 hours. We already knew from prior experiments in infected HeLa cells that nuclear egress is observed at 6 hpi, that viral particles reach the TGN at 12 hpi, and significant amounts of *de novo* virus are detected 18 hpi in the supernatant [202]. Thus, chelators were added at 4 hpi (prior to nuclear egress), 6 hpi (during nuclear egress), 12 hpi (virion maturation at the TGN) and 16 hpi (late stages of egress) to determine calcium requirements at those key events during viral egress. When viral titers were measured by plaque assays, we observed a significant decrease of viral load in the supernatant when infected cells were treated with Bapta-AM at early time points (figure 7). Indeed, at 4 and 6 hpi, 10 µM of Bapta-AM reduced the viral load by 94% and 84% while 20 µM of Bapta-AM caused 96% and 81% reduction respectively. Interestingly, there was an increase of 42% and 30% in the viral load when both concentrations of Bapta-AM were added at 16 hpi respectively. At those late times, the data were not statistically significant due to variation in the results obtained. Nonetheless, the results suggested that intracellular calcium may be critical early during nuclear egress. As for the EGTA treatment, it seemed that chelating extracellular calcium had no effect on the viral titer at each time points. In fact, the viral titer of EGTA-treated cells were at similar level as the mock-treated condition (figure 7).

When the cell lysate fraction of each condition was titrated, we observed a dose-dependent inhibitory as 10 and 20 µM Bapta-AM reduced viral titer by 40% and 95% at 4 hpi and by 49% and 79% at 6 hpi respectively (Figure 8). In this case, the addition of Bapta-AM at 12 or 16 hpi for both concentrations had no significant impact on viral titers as they were only slightly lower than the mock-treated infected condition. Similar results were obtained from the EGTA

treatment as we observed a non-significant decrease at 6, 12 and 16 hpi. As for 4 hpi, we observed a notable but not statistically significant increase of 35% of the viral titers (figure 8). Therefore, EGTA did not seem to have an effect on the intracellular viral load. Overall, this suggests that cytoplasmic calcium is required for the early stage of egress, likely at the nuclear stage.

To further investigate the effect of calcium on HSV-1 egress, infected Hela cells were also treated with ionomycin. Ionomycin is an antibiotic which induces intracellular calcium elevation in mammalian cells [203]. Infected cells were treated with a non-cytotoxic concentration of ionomycin (2 μM) at the same time points as previously mentioned. The supernatants and cell lysates were harvested at 18 hpi, and viral titers were measured by plaque assays. From figure 7, we can see that increasing cytosolic calcium levels at 4, 6 and 12 hpi had almost no effect on extracellular viral titers as they were comparable to the control condition. At 16 hpi, we observed a non-significant increase by 29% of the viral titers in the supernatant. As for the intracellular viral load, each time points were at similar levels as the mock-treated control (figure 8). Those data suggest that elevated levels of calcium does not inhibit nor favour viral egress.

Taken together, chelation of intracellular calcium at early time points during the infection affected negatively viral egress whereas chelation of extracellular calcium had no significant effect. Oddly, increasing intracellular calcium levels also had no measurable impact on viral egress.

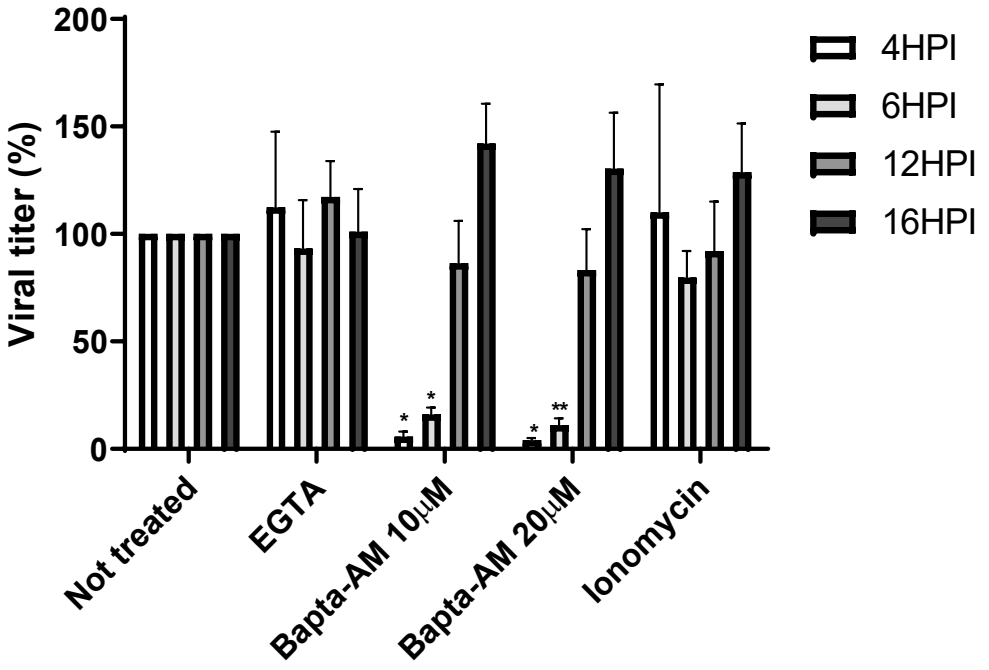

Fig 7. The viral titer is decreased in the supernatant when cytosolic calcium is chelated at early time point during viral egress

Hela cells were infected for 18 hours at a MOI of 2 with the thermosensitive virus V701. After 4 hpi at 39°C, the virus was released from the nucleus at 31°C for the subsequent 14 hours. Drugs were added at the indicated time points during the infection and kept in the media until harvesting. The supernatant of each condition was harvested at 18 hpi. Viral titers were measured by plaque assays (see Materials and Methods). Not treated cells were used as the normalized level of infection (100%). EGTA= 0.5 mM, ionomycin = 2 μM, Bapta-AM= 10 or 20 μM. n=3, error bars represent the SEM, statistical analysis by two-way ANOVA where *p* values are ≤ 0.05;*, ≤ 0.01; ** and ≤ 0.001; ***.

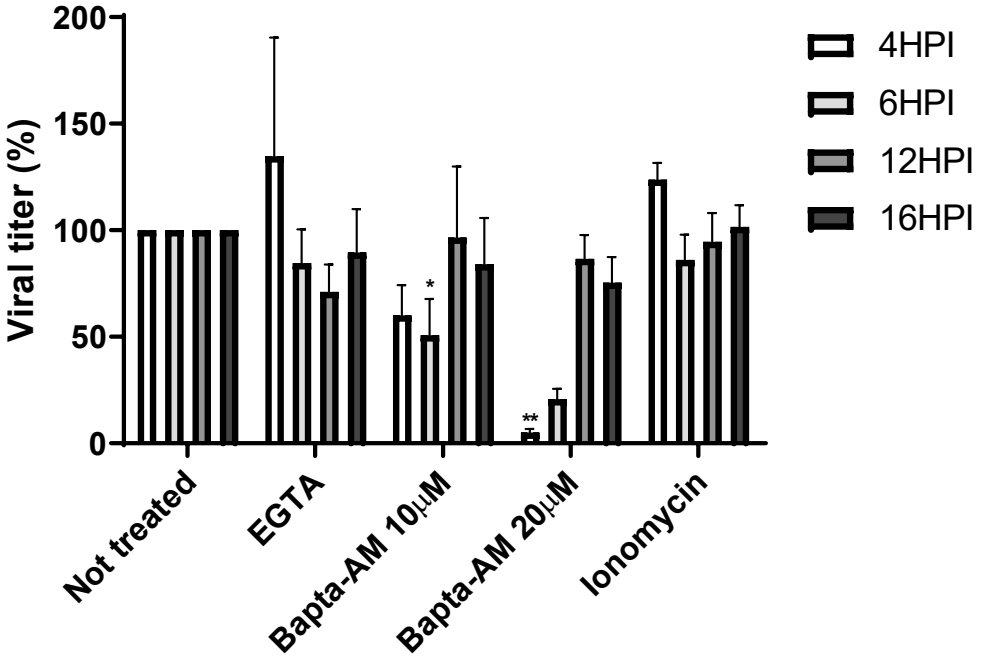

Fig 8. The viral titer is decreased in the cell lysate when cytosolic calcium is chelated at early time point during viral egress

Hela cells were infected for 18 hours at a MOI of 2 with the thermosensitive virus V701. After 4 hpi at 39°C, the virus was released from the nucleus at 31°C for the subsequent 14 hours. Drugs were added at the indicated time points during the infection and kept in the media until harvesting. The cell monolayer of each condition was harvested at 18 hpi. The viral titer was measured by plaque assays (see Materials and Methods). Untreated cells were used for normalization (100%). EGTA= 0.5 mM, ionomycin = 2 μM, Bapta-AM= 10 or 20 μM. n=3, error bars represent the SEM, statistical analysis by two-way ANOVA where p values are ≤ 0.05;*, ≤ 0.01; ** and ≤ 0.001; ***.

3.3. Chelation of Intracellular Calcium Early During Viral Egress Reduces Viral Genomic DNA Replication

Our previous results obtained by plaque assay demonstrated that chelation of intracellular calcium had a negative impact on HSV-1 egress. Although this method allowed us to measure viral titers, it can only detect infectious particles. In the next experiment, viral genomic DNA was measured by qPCR to determine the actual amount of newly synthesized viral particles in the supernatant. Since only one copy of viral genome is packaged into a capsid, we extrapolated that the amount of viral genomic DNA detected in the supernatant is equal to the amount of

newly synthesized mature virion. To perform this qPCR experiment, a gB expressing plasmid was used as control because this gene is present in one copy in the viral genome. Consistent with the above titration results, cells treated with Bapta-AM at early time points after viral entry showed a reduced amount of viral genomic DNA compared to mock-treated infected cells in the supernatant. In figure 9, viral copy number was reduced by 54% and 39% at 4 hpi and by 32% and 39% at 6 hpi for both Bapta-AM concentrations, respectively. Interestingly, the 4 and 6 hpi time points had similar amount of viral DNA and the dose dependant effect was no longer observed. At 12 and 16 hpi, the amount of viral DNA increased by 26% and 74% for 10 µM Bapta-AM and 29% and 94% for 20 µM Bapta-AM. Again, large data variation prevented us from detecting statistical differences regarding late time points. Similarly to titration experiments, EGTA did not have an impact on the amount of newly synthesized viral DNA (figure 9). When we analyzed viral genome copy numbers in the supernatant for ionomycin treatment, we observed an increase at 6, 12 and 16 hpi (40%, 59% and 64% respectively). Those increases were surprising considering that viral titers weren't significantly affected following cytosolic calcium elevation (figure 7 and 9). For 6 hpi, the results obtained frequently varied, which indicates that the difference between groups was not significant.

When probing the viral genomic DNA in the cell fractions (figure 10), EGTA did not seem to significantly alter the amount of viral DNA while 10 µM and 20 µM Bapta-AM greatly reduced the amount of viral DNA detected at early time points. On the other hand, the amount of viral DNA at 12 and 16 hpi for both Bapta-AM concentrations were either at the same level or slightly lower than the control conditions (figure 10). As for ionomycin, there were no significant differences between the control condition and the 4, 6 and 12 hpi time points in the cell fractions (figure 10). We did observe a 53% increase at 16 hpi from the cell lysate fractions, but this result was not statistically significant (figure 10).

Altogether, qPCR data demonstrated that early intracellular calcium chelation during viral egress negatively affects the amount of newly synthesized viral DNA released in the supernatant and in cell lysate. Those data are, in fact, supporting the trend observed from titration assays. In contrast, chelation of extracellular calcium had no effect on viral production for both fractions. As for ionomycin, it seemed that it promoted viral release in the supernatant at later time points,

but its effect remains unclear at early time points. For the cell lysate portion, cytosolic calcium elevation mostly had no effect.

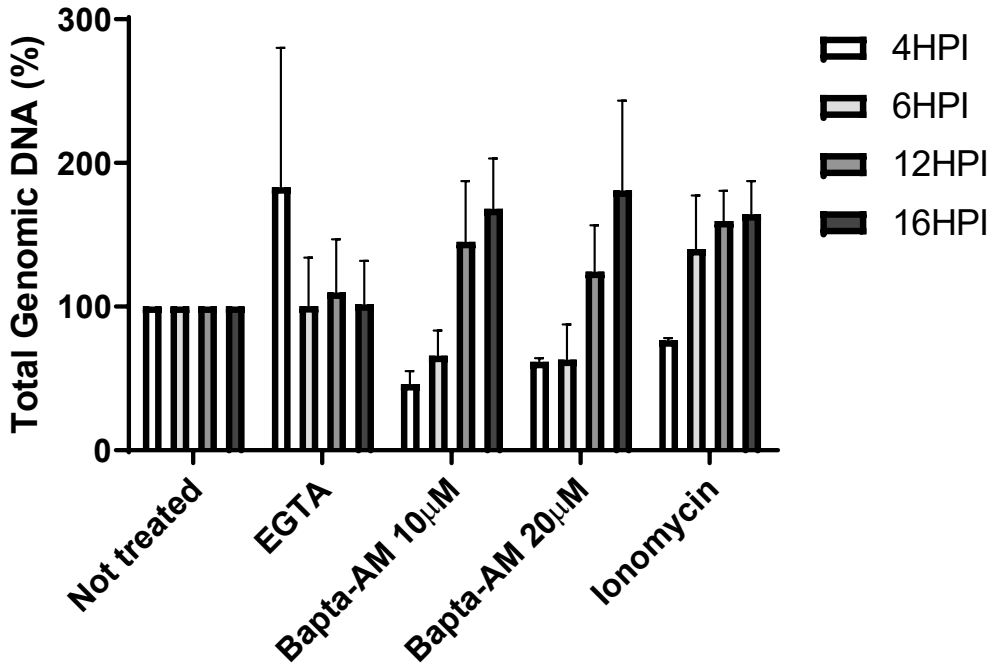

Fig 9. Chelation of cytosolic calcium reduces the amount of newly synthesized viral DNA in the supernatant

Hela cells were infected at a MOI of 2 with the thermosensitive virus V701. After 4 hpi at 39°C, the virus was released from the nucleus at 31°C for another 14 hours. Drugs were added at the indicated time points during the infection and kept in the media until harvesting. All supernatants were harvested at 18 hpi. Viral genomic DNA from viral particles in the supernatant was isolated then quantified by qPCR (see Materials and Methods). The gene of reference was gB. Untreated cells were used as controls (100%). EGTA (0.5 mM), ionomycin (2 μM), Bapta-AM (10 or 20 μM). n=3, error bars represent the SEM, statistical analysis by two-way ANOVA. No statistically significant differences were noted.

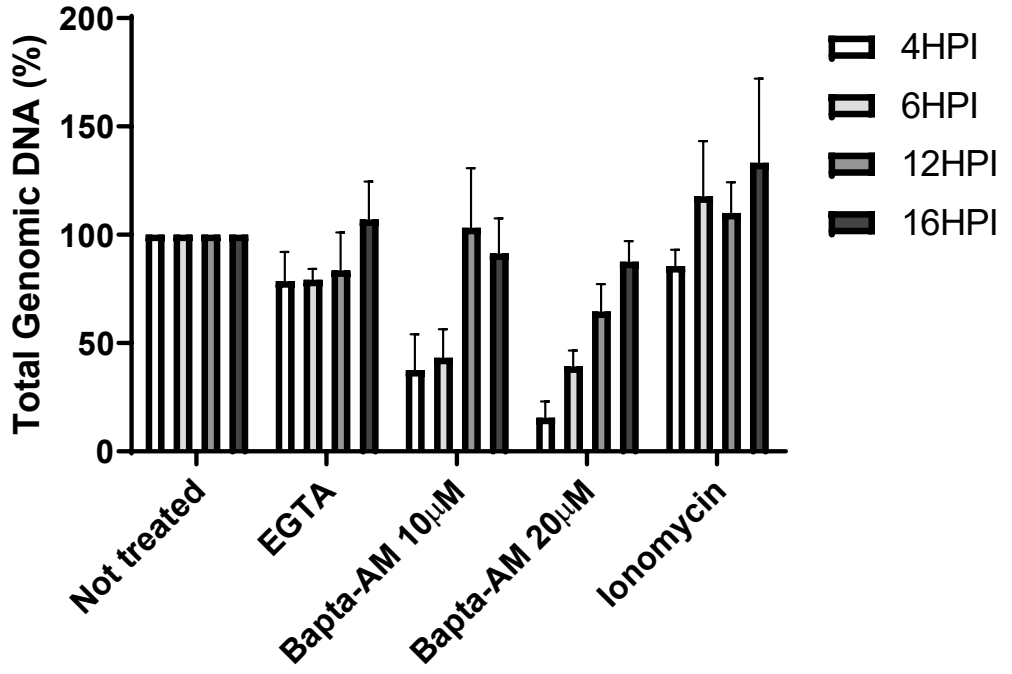

Fig 10. Chelation of cytosolic calcium reduces the amount of newly synthesized viral DNA in the cell lysate fraction

Hela cells were infected for 18 hours at a MOI of 2 with the thermosensitive virus V701. After 4 hpi at 39°C, the virus was released from the nucleus for the subsequent 14 hours. Drugs were added at the indicated time points during the infection and kept in the media until harvesting. The supernatant of each condition was harvested at 18 hpi. Viral genomic DNA from the cell lysate was isolated then quantified by qPCR (see Materials and Methods). The gene of reference was gB. Untreated cells were used as controls (100%). EGTA (0.5 mM), ionomycin (2 μM), Bapta-AM (10 or 20 μM). n=3, error bars represent the SEM, statistical analysis by two-way ANOVA. No statistically significant differences were noted.

In a typical HSV-1 stock, about 1 in 10 viral particles is infectious. Changes in this ratio following drug treatment may imply that modifying the calcium concentration affects viral infectivity. In order to determine if infectivity of newly synthesized HSV-1 particles is altered following each treatment, viral particle infectivity was assessed by dividing viral titers by viral genomic copy numbers. Mock-treated infected cells were set as the basal infectivity and used to normalize the other conditions. Hence, values over 100% imply an increased infectivity while values under 100% suggest a decrease in infectivity compared to the control condition. When we analyzed data from the supernatants, we observed a significant dose-dependent decrease in the pfu/genome copy ratio of viruses produced by cells treated with both concentrations of

Bapta-AM at 4 and 6 hpi (figure 11). This suggested that not only chelating intracellular calcium at early time points resulted in a lower viral production, but that it also generated less infectious particles. In agreement with previous results, this ratio remained statistically unaffected at 12 and 16 hpi at both Bapta-AM concentrations (figure 11). Regarding the EGTA and ionomycin treatments, the same trends was once again observed since they both had no significant effect on viral infectivity (figure 11). When we analyzed the cell lysate fractions, EGTA and ionomycin treatments remained consistent with their negligible effect on the viral pfu/genome ratio throughout the different stages of infection (figure 12). As for 10 µM Bapta-AM, its early addition during egress surprisingly resulted in viral particles that had statistically equivalent infectivity as those from untreated cells at all times. On the other hand, 20 µM Bapta-AM treatment reduced, as expected, viral particles infectivity (figure 12).

In summary, cytosolic calcium chelation reduced viral particle infectivity in the supernatant when it occurs early during egress, while EGTA and ionomycin did not have an effect on the pfu/viral genome ratio in both cellular and extracellular fractions at all time points.

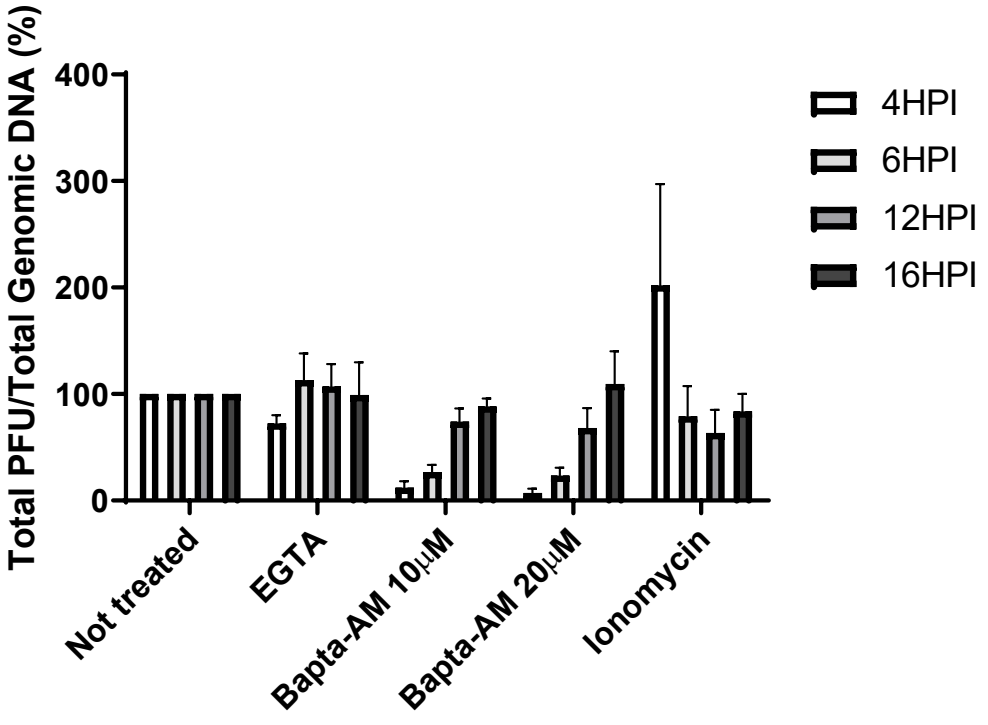

Fig 11. Changes in the cytosolic calcium level affect the infectivity ratio of newly synthesized viral particles released in the supernatant

To determine the infectivity ratio of newly synthesized viruses from each condition, the total pfu was divided by the viral genomic copy number (See methods section). The untreated condition was used to normalize the data as it represents the basal infectivity level of the virus. Value greater or lower than 100% signify that there were more or less infectious particles produced for the same amount of genomic DNA released in the supernatant, respectively. EGTA (0.5 mM), ionomycin (2 μM), Bapta-AM (10 or 20 μM). n=3, error bars represent the SEM, statistical analysis by two-way ANOVA. No statistically significant differences were noted.

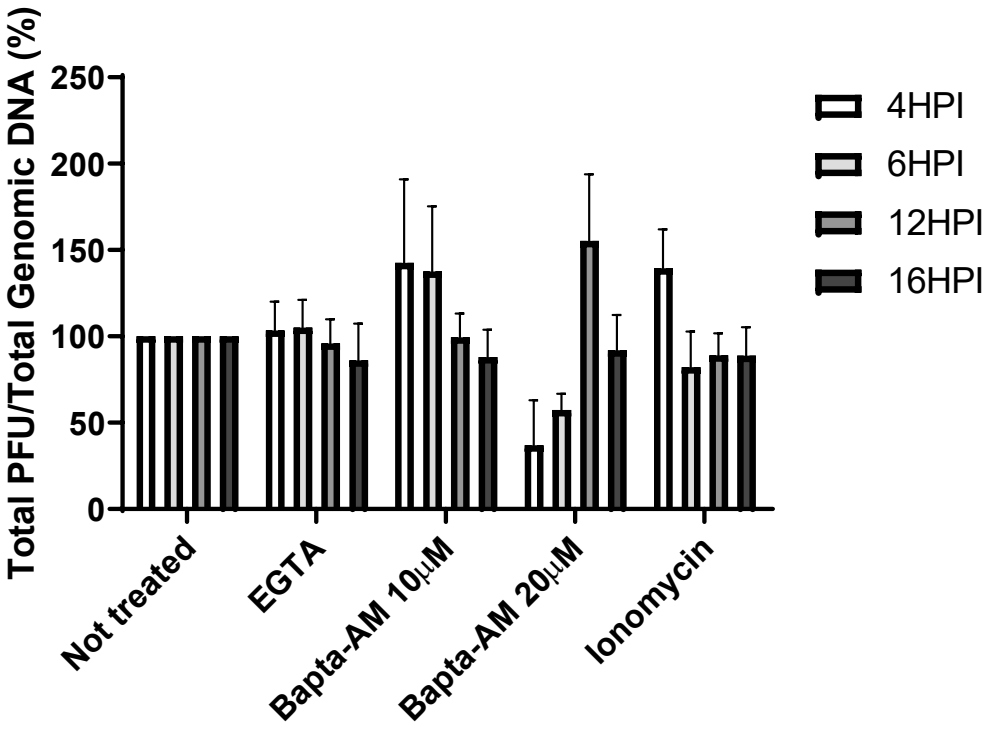

Fig 12. Changes in the cytosolic calcium level affect the infectivity of newly synthesized viral particles released in the cell lysate fraction

To determine the infectivity of newly synthesized viruses of each condition, the total pfu was divided by the viral genomic DNA (See methods section). The untreated condition was used to normalize the data as it represented the basal infectivity level of the virus. Value greater or lower than 100% signify that there were more or less infectious particles produced for the same amount of genomic DNA released in the supernatant, respectively. EGTA (0.5 mM), ionomycin (2 μM), Bapta-AM (10 or 20 μM). n=3, error bars represent the SEM, statistical analysis by two-way ANOVA. No statistically significant differences were noted.

We thus demonstrated that the presence of calcium was required during nuclear egress at early time points as it diminished viral production and infectivity ratio when sequestered by intracellular chelators. In contrast, sequestering intracellular calcium at 12 and 16 hpi did not have any significant effect. Therefore, those data suggest that HSV-1 nuclear egress is closely linked to cytosolic calcium homeostasis. We previously demonstrated that E-Syt1, a calcium-sensing ER-PM tethering protein, modulates viral egress negatively [153]. As the function of E-Syt1 is activated by elevated calcium level, and it would probably be inactivated in presence of Bapta-AM, it is interesting to note that sequestering calcium at 16 hpi had no effect on viral egress. To evaluate the possible implication of E-Syt1on viral egress, the inhibitory effect of E-Syt1 was further investigated using E-Syt1 mutants. As explained earlier, mutations in key domains render those mutants unable to sense cytosolic calcium or bind to phospholipids at the PM. Hence, the objective of our next experiments was to determine if E-Syt1 mutants are able to alleviate the negative regulatory effect of overexpressed wild-type E-Syt1 on viral egress.

3.4. Mutants of E-Syt1 Do Not Induce Viral Titer Recovery

To start our investigation, the viability of Hela cells overexpressing the different E-Syt1 constructs was assessed using the Alamar blue assay. As shown in figure 13, cell viability was not impaired by overexpressing the different forms of E-Syt1. Next, E-Syt1WT and mutants were overexpressed in infected Hela cells to determine their effect on viral egress. As stated previously, the first mutant, E-Syt1 (7x), has seven point mutations at its calcium sensing domain (C2C) which disrupt its ability to bind to calcium [193]. As for the second mutant, E-Syt1 ΔC2E, it has its entire C2E domain deleted which prevents it from interacting with PI(4,5)P2 lipids at the PM and tether the ER to the PM [193]. In order to make comparative analyses between each construct, we first had to confirm that all constructs were expressed at similar levels inside Hela cells. To do so, a western blot was performed using the cell lysate of each condition. E-Syt-1 WT and (7x) were detected with an anti-E-Syt1 while E-Syt1 ΔC2E was detected with anti-GFP since the anti-E-Syt1's epitope is located in the C2E domain (Bethyl Laboratory). As shown in figure 14, E-Syt-1 WT and (7x) were expressed at similar levels, and their expression levels were greater than the endogenous E-Syt1. As for E-Syt1 ΔC2E, we could

not compared its expression level to the other E-Syt1 mutants because we could not find a suitable common antibody. Since all plasmid containing E-Syt1 mutants had the same backbone, it is likely that E-Syt1 ΔC2E was also expressed at similar level as the other mutants. Nonetheless, we were able to confirm that all overexpressed proteins were at the right molecular weight.

We previously demonstrated in an entry assay that E-Syt1 down regulation increased HSV-1 infection [153]. To be able to observe the post-entry effect of overexpressed E-Syt1 on viral egress, infected cells were treated with phosphonoacetic acid (PAA), a specific viral DNA polymerase inhibitor, to enable viral entry but block egress [204, 205]. Following transfection, this drug was removed when the construct of interest was expressed. Briefly, Hela cells were infected with HSV-1 17+ WT virus at a MOI of 2. After 1h of absorption, cells were treated with 0.2 µg/ml PAA then transfected with E-Syt1 WT, E-Syt1 (7x) or E-Syt1 ΔC2E at 12 hpi. As transfection controls, the transfection agent only and a plasmid expressing only GFP (GFP-N2) were used. After 24 hpi, media containing PAA was replaced by fresh media to remove the PAA and allow viral egress for an additional 18 hours. The supernatants and cell lysates were harvested as mentioned in the methods section, then viral titers were measured by titration. By analyzing the titration data from figure 15, we can see that E-Syt1 WT and E-Syt1 ΔC2E overexpression had no inhibitory effect on viral egress in the supernatant. Indeed, viral titers from E-Syt1 WT and E-Syt1 ΔC2E conditions were comparable to the lipofectamine 3000 (control) condition. As for the E-Syt1 (7x) mutant, the decrease in viral titers was not significant as the GFP control also resulted in a similar decrease in viral titers. When we looked at the cell lysate fractions (figure 16), a similar trend was observed for E-Syt1 WT and E-Syt1 ΔC2E conditions as no significant inhibitory effect were detected. Although we observed a statistically significant reduction of viral titer for the E-Syt1 (7x) condition, we cannot conclude that this mutant impaired viral egress. Indeed, as the supernatant fraction, we observed an inhibitory effect from GFP-expressing cells on viral titer. Consequently, all constructs did not result in a significant effect on viral egress in both fractions. Altogether, we were not able to detect any significant inhibitory effect resulting from overexpressing E-Syt1 WT or mutants in both fractions of infected Hela cells.

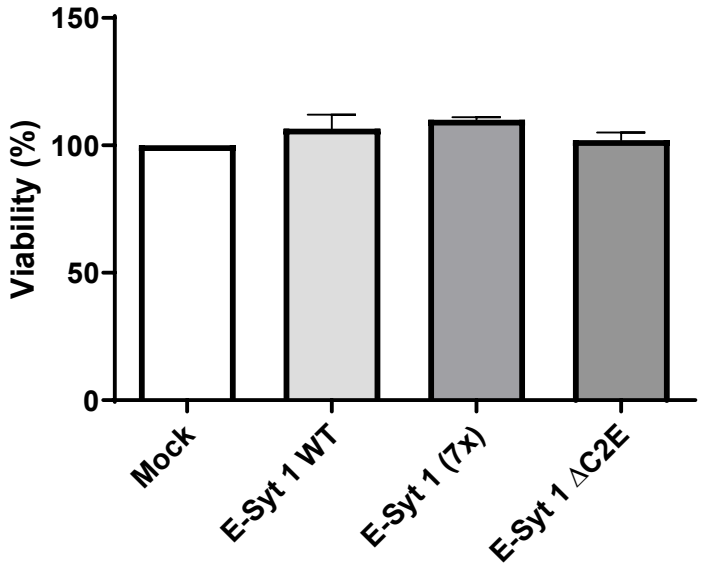

Fig 13. Overexpression of the different constructs of E-Syt1 does not affect cell viability

Hela cells were transfected with E-Syt1 WT, 7x or ΔC2E construct. After 19 hours, Alamar blue was added to the media of each condition and fluorescence was measured 25 hours post transfection. Each measurement was performed in triplicate and the average of three independent experiments is represented. Error bars represent the SEM and statistical analysis was performed by one-way ANOVA. No statistically significant differences were noted.

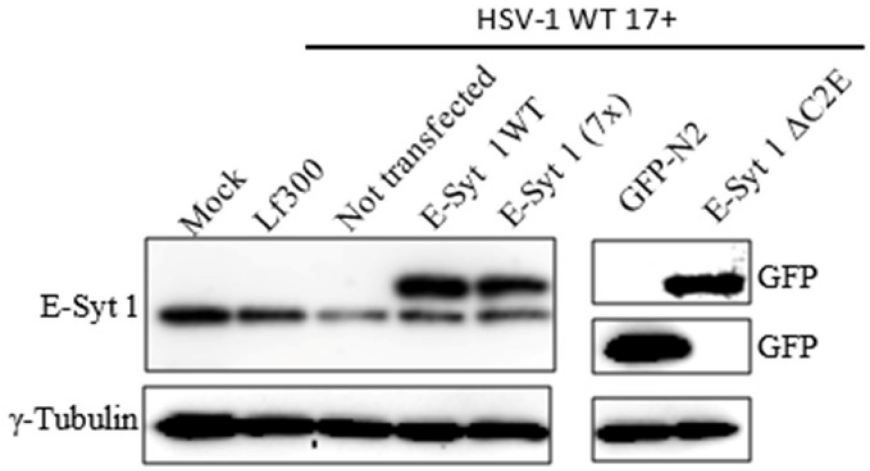

Fig 14. The different E-Syt1 constructs are expressed at similar level

Hela cells were infected with HSV-1 17+ WT virus then transfected with plasmid containing E-Syt1 WT, E-Syt1 (7x), E-Syt1 ΔC2E or GFP. Mock represents cells that were neither transfected nor infected. Lf3000 represents cells that were treated with Lipofectamine 3000 (the transfection agent) and infected while the untransfected condition represents cells that were infected only. Thirty micrograms of proteins from each condition was loaded on an SDS-PAGE gel and transferred on a PVDF membrane. Proteins of interest were detected using the indicated antibody. In the above figure, we can see the overexpressed protein E-Syt1 WT (150 kDa), E-Syt1 (7x) (152 kDa) and the endogenous protein E-Syt 1 (123 kDa). E-Syt1 ΔC2E (136 kDa) was detected using anti-GFP because the anti-E-Syt1's epitope is within the deleted C2E domain.

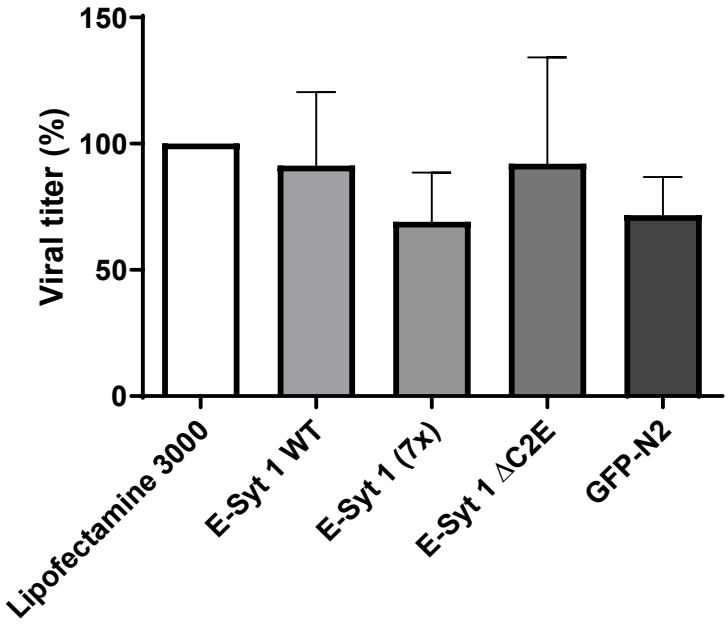

Fig 15. Overexpression of the different E-Syt1 mutants did not inhibit viral egress in the supernatant of infected Hela cells

The supernatant of infected-transfected Hela cells was harvested at 24 hpi. Viral titers were measured by plaque assays and normalized on infected cells treated with only the transfecting agent. n=3, error bars represent the SEM, statistical analysis by one-way ANOVA. No statistically significant differences were noted.

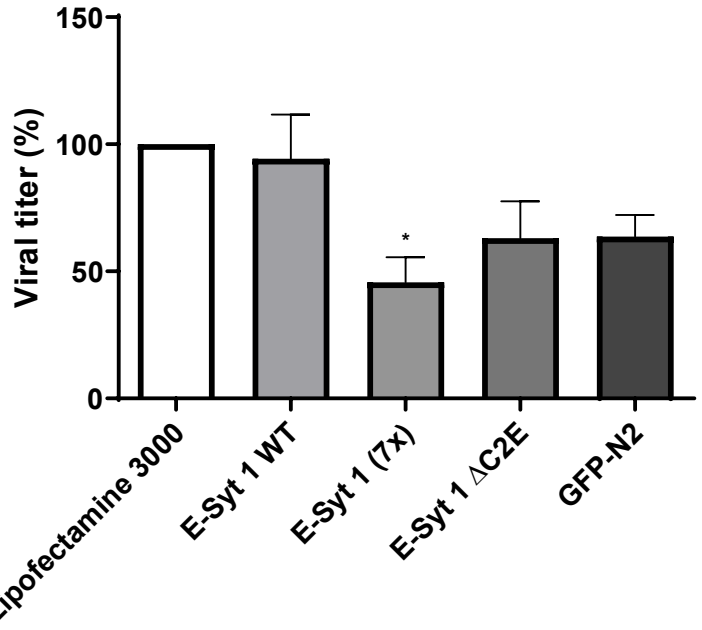

Fig 16. Overexpression of the different E-Syt1 mutants did not inhibit viral egress in the cell lysate of infected Hela cells

The cell lysate of infected-transfected Hela cells was harvested at 24 hpi. Viral titers were measured by plaque assays and normalized on infected cells treated with only the transfecting agent. n=3, error bars represent the SEM, statistical analysis by two-way ANOVA where *p* values are ≤ 0.05;*, ≤ 0.01; ** and ≤ 0.001; ***.

4. Discussion

It was previously demonstrated that HSV-1 triggers an increase in cytosolic calcium during viral entry [188]. This increase of calcium was found to be necessary to perform proper infection as depletion of cytosolic calcium didn't prevent attachment of viral particles to their receptors but inhibited penetration into the cell [190]. In the present study, we investigated the requirement of calcium for viral egress given the implication of the E-Syt1 calcium sensing protein during this step [153]. Taking into account that viral particles have to bypass similar barriers during egress than entry, and that calcium regulates many cellular processes, we hypothesized that calcium plays a role during viral egress. Data from this study demonstrate that sequestering intracellular calcium at 4 and 6 hpi had a negative impact on viral propagation in both the supernatant and cell lysate (figures 7 and 8). Additionally, newly synthesized viral particles had a diminished infectivity ratio when the intracellular calcium chelator Bapta-AM was added at early time points during nuclear egress (figures 11 and 12). Those phenotypes strongly suggest that cytosolic calcium is required as soon as 4 and 6 hpi. However, we did not see any major accumulation nor misallocation of viral particles in the presence of any drugs (figure 6). It may be that the changes are too subtle to notice without quantifying the immunofluorescence images. More likely, it may simply be that although an equivalent number of viral particles were produced, a smaller proportion of those particles were infectious. This hypothesis is supported by our pfu/viral genome copy data (figures 11 and 12). Importantly, this intracellular calcium requirement was independent of E-Syt1's calcium sensing function as overexpressing E-Syt1 (7x) had no significant effect on the viral egress (figures 15 and 16).

An important issue is the reduced infectivity ratio of viral particles that are produced (figures 11 and 12). This phenomenon might be explained by the fact that Bapta-AM disrupts ER homeostasis which, in turn, may affect post-translational modifications of viral proteins [206, 207]. In fact, ER homeostasis is regulated by the level of misfolded protein and calcium concentration in the ER lumen. When homeostasis is disrupted, it generates a stress on the ER that activates the unfolded protein response (UPR) mechanism. UPR signalling induces three pathways (PERK, IRE1, and ATF6 pathways) whose activity results in protein translation shutdown, mRNA degradation, misfolded protein degradation, induction of ER-Ca^{2+} refilling

and increase in chaperone activity [208]. It is noteworthy to mention that calcium binds and activates chaperones and folding enzymes, and that decreasing ER-Ca^{2+} concentration enhances misfolded protein accumulation and triggers UPR [206]. During lytic infection, massive synthesis of viral proteins causes ER stress due to accumulation of unfolded proteins [209]. However, HSV-1 has evolved mechanisms to counteract the action of UPR pathways and ensure the proper synthesis/maturation of its viral proteins. For example, γ1 34.5 induces the dephosphorylation of eIF-2α while U_S11 represses PKR activity [210, 211]. In our experiment, HSV-1 was probably able to alleviate the detrimental effect of UPR on its propagation, but the decrease in calcium by Bapta-AM might have prevented the proper function of chaperones and folding enzymes. Consequently, more defective viral particles may have been produced. It would be interesting to investigate if those processes were indeed induced and if they resulted in accumulation of more misfolded viral proteins. The Asano laboratory has observed a decrease in the transport of glycosylated viral glycoproteins to the Golgi when BHK and Hela cells were infected with vesicular stomatitis virus (VSV) and ER homeostasis was disrupted by 5 μM ionomycin. Indeed, VSV-G remains associated with calnexin during the infection, showing that calcium plays a role in protein maturation [212]. Interestingly, in our experiment, increasing cytosolic calcium levels at early time points with ionomycin had no detectable effect on viral egress. We must mention that in our study, cells were treated with 2 μM ionomycin, which might not be enough to induce a detectable effect on the viral egress. It would be interesting to perform calcium imaging studies to monitor changes in calcium level inside cells throughout viral egress in presence or absence of Bapta-AM and ionomycin. Such experiments would imply employment of calcium indicator to record calcium concentration fluctuations over the course of HSV-1 egress. Additionally, determining the effect of Bapta-AM and ionomycin on viral protein maturation at 4 and 6 hpi would also give us great insight on calcium requirements during HSV-1 egress. In fact, it was reported that post-translational N-glycosylation of viral glycoproteins, which primarily occurs at the ER, is essential to produce infectious mature virions [213-216]. In this experiment, we would be able to monitor accumulation of immature glycoproteins following calcium homeostasis disturbance. Other researchers also observed decrease in viral yield when calcium homeostasis was disrupted with pharmaceutical drugs [217]. Those drugs did not only prevented proper viral entry but decreased viral maturation and

budding from infected cells. Although those data were acquired from experiments using other DNA and RNA viruses, it demonstrates that calcium-associated mechanisms are commonly modulated by viruses to enable proper propagation.

When added late during the infection, Bapta-AM and ionomycin caused a not statistically significant increase in viral load in the supernatant (figures 7 and 9). As those drugs have an opposite effect on cytosolic calcium concentrations, we were expecting to see an opposite effect on viral egress. In the literature, it is not clear how an increase or decrease of cytosolic calcium concentrations can favour release of HSV-1 particles. It was suggested that low calcium levels stabilize microtubules (i.e. in the presence of Bapta-AM), which should promote transport of new particles to the plasma membrane [218-220]. Conversely, an increase of calcium promotes Rab proteins activity that are also implicated in the secretory pathway used by HSV-1 [221, 222]. Consequently, our current knowledge on cellular and molecular processes cannot explain the phenomenon observed at later time points for both Bapta-AM and ionomycin.

Earlier work by the laboratory revealed that E-Syt1 down regulation by RNA interference stimulated viral release while overexpressing E-Syt1 in infected cells decreased viral yield [153]. However, contradictory results were obtained in the present study as overexpressing wild type E-Syt1 did not inhibit HSV-1 egress (figures 15 and 16). As for the mutants, we did not observe any specific effect on the viral egress given that the transfection control, GFP-N2, had a similar inhibitory effect (figures 15 and 16). This phenomenon might be explained by the fact that transitory transfection triggers the cellular innate immune system, specifically the type I interferon (IFN) pathway [223-225]. Consequently, it would result in less virus produced. On the other hand, HSV-1 has evolved many mechanisms to evade the host defence system [226]. Therefore, it is surprising that transitory transfection (regardless of the gene expressed) induces the inhibition of viral propagation post-entry. To bypass the unexpected effect of transfection on viral egress, it would be interesting to repeat those experiments in cells that stably express the different E-Syt1's mutants.

Although this study was done rigorously, some limitations were encountered in the experiments. The first limitation that we experienced was the expression of E-Syt1 mutants in infected cells. In fact, many attempts using different protocols were performed to obtain a cell population that was mutually overexpressing E-Syt1 mutants while enabling HSV-1 infection.

Some preliminary data using IF demonstrated that overexpressing E-Syt1 Hela cells were not able to be infected while infected cells were not expressing the constructs. Therefore, only a small portion of the cell population was transfected and infected. This limitation was not exclusive to E-Syt1 proteins as we encountered the same issue with the GFP control. It is important to mention that each technique was performed and validated separately to exclude the manipulation issues. It was hypothesized that the innate response might be the cause of this limitation. Thus, we tried to transfect and infect Vero cells, which do not produce type I interferon [227, 228]. Despite the use of several transfection agents and protocols, we were not able to successfully transfect Vero cells. As an alternative, we used PAA to temporarily halt HSV-1 replication, and allow E-Syt1 mutants overexpression prior to the release of HSV-1 from the nucleus. Even if not all cells were transfected and infected, this method was the most suitable as it resulted in 50% of cells that were transfected and infected. Since the other half of the population is a mixture of transfected or infected cells, it remains difficult to make any conclusion from those experiments. As stated earlier, it will be interesting to repeat those experiments with using Hela cells stably expressing E-Syt1 mutants. Those cell lines could be generated by using an inducible system that will initiate the expression of E-Syt1 mutants only when cells are infected.

The other limitation that we encountered throughout this study is the wide variation in the data set. Indeed, we obtained large standard error of the mean (SEM) values, which is depicted by large error bars in most figures (figure 7-12, 15, 16). This situation results from small sample size as each experiment was performed in triplicate (n=3). To solve this problem, we should use a larger sample size. Since the SEM is sensitive to the n value, larger sample size would reduce variation within each experimental condition. The lack of statistical significance in some results that seem to have a noticeable effect can also be explained by the small sample size. Indeed, ANOVA analysis is also influenced by the sample size as it is sensitive to variation within a group [229, 230]. Therefore, increasing our sample size would allow us to draw better conclusions as data would represent phenomenon seen in a larger population and allows us to obtain more robust statistical analysis.

5. Conclusion

From results obtained in this study, we can conclude that intracellular calcium plays an important role during the early egress stage of HSV-1 propagation. In fact, treatment with the cytosolic calcium chelator Bapta-AM at 4 and 6 hpi resulted in a significant and reproducible decrease of viral titers in supernatants and cell lysates. In addition, newly synthesized viral particles from cells treated with Bapta-AM at 4 and 6 hpi had a lower infectivity ratio. Those data imply that cytosolic calcium is involved in many early processes that mediate viral particle egress and infectivity. Since calcium sensing by E-Syt1 did not explain these results, ER homeostasis was hypothesized as one factor that might affect viral propagation early during the infection. As for later time points, further investigation is required to elucidate what is going on at the plasma membrane level.

6. Bibliography

1. Whitley, R.J., *Herpesviruses*, in *Medical Microbiology*, S. Baron, Editor. 1996, University of Texas Medical Branch at Galveston.: Galveston (TX).

2. Cruz-Muñoz, M.E. and E.M. Fuentes-Pananá, *Beta and Gamma Human Herpesviruses: Agonistic and Antagonistic Interactions with the Host Immune System.* Frontiers in microbiology, 2018. **8**(2521): p. 1-20.

3. Looker, K.J., et al., *Global and Regional Estimates of Prevalent and Incident Herpes Simplex Virus Type 1 Infections in 2012.* PLOS ONE, 2015. **10**(10): p. 1-17.

4. Menendez, C.M. and D.J.J. Carr, *Defining nervous system susceptibility during acute and latent herpes simplex virus-1 infection.* Journal of neuroimmunology, 2017. **308**: p. 43-49.

5. Maroui, M.A., et al., *Latency Entry of Herpes Simplex Virus 1 Is Determined by the Interaction of Its Genome with the Nuclear Environment.* PLOS Pathogens, 2016. **12**(9): p. 1-28.

6. Shaikh, A.G., et al., *The floccular syndrome in herpes simplex type 1 encephalitis.* Journal of the Neurological Sciences, 2013. **325**(1): p. 154-155.

7. Livorsi, D., et al., *Brainstem encephalitis: an unusual presentation of herpes simplex virus infection.* Journal of Neurology, 2010. **257**(9): p. 1432-1437.

8. Kaye, S. and A. Choudhary, *Herpes simplex keratitis.* Progress in Retinal and Eye Research, 2006. **25**(4): p. 355-380.

9. Eimer, W.A., et al., *Alzheimer's Disease-Associated β-Amyloid Is Rapidly Seeded by Herpesviridae to Protect against Brain Infection.* Neuron, 2018. **99**(1): p. 56-63.

10. Itzhaki, R.F., *Corroboration of a Major Role for Herpes Simplex Virus Type 1 in Alzheimer's Disease.* Frontiers in aging neuroscience, 2018. **10**: p. 324-324.

11. Gupta, K. and R. Metgud, *Evidences Suggesting Involvement of Viruses in Oral Squamous Cell Carcinoma.* Pathology Research International, 2013. **2013**: p. 1-17.

12. Jain, M., *Assesment of Correlation of Herpes Simplex Virus-1 with Oral Cancer and Precancer- A Comparative Study.* Journal of clinical and diagnostic research : JCDR, 2016. **10**(8): p. 14-17.

13. Starr, J.R., et al., *Serologic Evidence of Herpes Simplex Virus 1 Infection and Oropharyngeal Cancer Risk.* Cancer Research, 2001. **61**(23): p. 8459-8464.

14. McGeoch, D.J., *The Genome of Herpes Simplex Virus: Structure, Replication and Evolution.* Journal of Cell Science, 1987. **1987**(Supplement 7): p. 67-94.

15. Karamitros, T., et al., *De Novo Assembly of Human Herpes Virus Type 1 (HHV-1) Genome, Mining of Non-Canonical Structures and Detection of Novel Drug-Resistance Mutations Using Short- and Long-Read Next Generation Sequencing Technologies.* PLOS ONE, 2016. **11**(6): p. 1-19.

16. Roizman, B., *The structure and isomerization of herpes simplex virus genomes.* Cell, 1979. **16**(3): p. 481-494.

17. Strang, B.L. and N.D. Stow, *Circularization of the Herpes Simplex Virus Type 1 Genome upon Lytic Infection.* Journal of Virology, 2005. **79**(19): p. 12487-12494.

18. Szpara, M.L., et al., *Evolution and Diversity in Human Herpes Simplex Virus Genomes.* Journal of Virology, 2014. **88**(2): p. 1209-1227.

19. Rock, D.L. and N.W. Fraser, *Latent herpes simplex virus type 1 DNA contains two copies of the virion DNA joint region.* Journal of virology, 1985. **55**(3): p. 849-852.

20. Su, Y.-H., et al., *Evidence that the Immediate-Early Gene Product ICP4 Is Necessary for the Genome of the Herpes Simplex Virus Type 1 ICP4 Deletion Mutant Strain d120 To Circularize in Infected Cells.* Journal of Virology, 2006. **80**(23): p. 11589-11597.

21. Macdonald, S.J., et al., *Genome Sequence of Herpes Simplex Virus 1 Strain KOS.* Journal of Virology, 2012. **86**(11): p. 6371-6372.

22. Watson, Z., et al., *Role of Polycomb Proteins in Regulating HSV-1 Latency.* Viruses, 2013. **5**(7): p. 1740-1757.

23. Liu, Y.-T., et al., *Cryo-EM structures of herpes simplex virus type 1 portal vertex and packaged genome.* Nature, 2019. **570**(7760): p. 257-261.

24. Bowman, B.R., et al., *Structure of the herpesvirus major capsid protein.* The EMBO journal, 2003. **22**(4): p. 757-765.

25. Dai, X. and Z.H. Zhou, *Structure of the herpes simplex virus 1 capsid with associated tegument protein complexes.* Science, 2018. **360**(6384): p. 1-12.

26. Sugimoto, K., et al., *Simultaneous Tracking of Capsid, Tegument, and Envelope Protein Localization in Living Cells Infected with Triply Fluorescent Herpes Simplex Virus 1.* Journal of Virology, 2008. **82**(11): p. 5198-5211.

27. Lv, Y., et al., *Remodeling of host membranes during herpesvirus assembly and egress.* Protein & Cell, 2019. **10**(5): p. 315-326.

28. Turcotte, S., J. Letellier, and R. Lippé, *Herpes Simplex Virus Type 1 Capsids Transit by the trans-Golgi Network, Where Viral Glycoproteins Accumulate Independently of Capsid Egress.* Journal of Virology, 2005. **79**(14): p. 8847-8860.

29. Owen, D.J., C.M. Crump, and S.C. Graham, *Tegument Assembly and Secondary Envelopment of Alphaherpesviruses.* Viruses, 2015. **7**(9): p. 5084-5114.

30. Abaitua, F., et al., *A Nuclear localization signal in herpesvirus protein VP1-2 is essential for infection via capsid routing to the nuclear pore.* Journal of virology, 2012. **86**(17): p. 8998-9014.

31. Kelly, B.J., et al., *The interaction of the HSV-1 tegument proteins pUL36 and pUL37 is essential for secondary envelopment during viral egress.* Virology, 2014. **454-455**: p. 67-77.

32. Diefenbach, R.J., *Conserved tegument protein complexes: Essential components in the assembly of herpesviruses.* Virus Research, 2015. **210**: p. 308-317.

33. Kelly, B.J., et al., *Functional roles of the tegument proteins of herpes simplex virus type 1.* Virus Research, 2009. **145**(2): p. 173-186.

34. Zhang, J., et al., *Early, Active, and Specific Localization of Herpes Simplex Virus Type 1 gM to Nuclear Membranes.* Journal of Virology, 2009. **83**(24): p. 12984-12997.

35. El Kasmi, I. and R. Lippe, *Herpes simplex virus 1 gN partners with gM to modulate the viral fusion machinery.* Journal of virology, 2015. **89**(4): p. 2313-2323.

36. Cooper, R.S. and E.E. Heldwein, *Herpesvirus gB: A Finely Tuned Fusion Machine.* Viruses, 2015. **7**(12): p. 6552-6569.

37. O'Donnell, C.D. and D. Shukla, *The Importance of Heparan Sulfate in Herpesvirus Infection.* Virologica Sinica, 2008. **23**(6): p. 383-393.

38. Spear, P.G., R.J. Eisenberg, and G.H. Cohen, *Three Classes of Cell Surface Receptors for Alphaherpesvirus Entry.* Virology, 2000. **275**(1): p. 1-8.

39. Spear, P.G., *Herpes simplex virus: receptors and ligands for cell entry.* Cellular Microbiology, 2004. **6**(5): p. 401-410.

40. Yoon, M., et al., *Mutations in the N Termini of Herpes Simplex Virus Type 1 and 2 gDs Alter Functional Interactions with the Entry/Fusion Receptors HVEM, Nectin-2, and 3-O-Sulfated Heparan Sulfate but Not with Nectin-1.* Journal of Virology, 2003. **77**(17): p. 9221-9231.

41. Reske, A., et al., *Understanding HSV-1 entry glycoproteins.* Reviews in Medical Virology, 2007. **17**(3): p. 205-215.

42. Gianni, T. and G. Campadelli-Fiume, *αVβ3-Integrin Relocalizes nectin1 and Routes Herpes Simplex Virus to Lipid Rafts.* Journal of Virology, 2012. **86**(5): p. 2850-2855.

43. Chowdary, T.K., et al., *Crystal structure of the conserved herpesvirus fusion regulator complex gH–gL.* Nature Structural & Molecular Biology, 2010. **17**: p. 882-888.

44. Arii, J., et al., *Nonmuscle Myosin Heavy Chain IIB Mediates Herpes Simplex Virus 1 Entry.* Journal of Virology, 2015. **89**(3): p. 1879-1888.

45. Walsh, D. and M.H. Naghavi, *Exploitation of Cytoskeletal Networks during Early Viral Infection.* Trends in Microbiology, 2019. **27**(1): p. 39-50.

46. Arii, J., et al., *Non-muscle myosin IIA is a functional entry receptor for herpes simplex virus-1.* Nature, 2010. **467**: p. 859-862.

47. Agelidis, A.M. and D. Shukla, *Cell entry mechanisms of HSV: what we have learned in recent years.* Future Virology, 2015. **10**(10): p. 1145-1154.

48. Gianni, T., G. Campadelli-Fiume, and L. Menotti, *Entry of Herpes Simplex Virus Mediated by Chimeric Forms of Nectin1 Retargeted to Endosomes or to Lipid Rafts Occurs through Acidic Endosomes.* Journal of Virology, 2004. **78**(22): p. 12268-12276.

49. Komala Sari, T., et al., *Contributions of Herpes Simplex Virus 1 Envelope Proteins to Entry by Endocytosis.* Journal of Virology, 2013. **87**(24): p. 13922-13926.

50. Copeland, A.M., W.W. Newcomb, and J.C. Brown, *Herpes Simplex Virus Replication: Roles of Viral Proteins and Nucleoporins in Capsid-Nucleus Attachment.* Journal of Virology, 2009. **83**(4): p. 1660-1668.

51. Chang, K., et al., *Filopodia and Viruses: An Analysis of Membrane Processes in Entry Mechanisms.* Frontiers in microbiology, 2016. **7**(300): p. 1-16.

52. Miranda-Saksena, M., et al., *Infection and Transport of Herpes Simplex Virus Type 1 in Neurons: Role of the Cytoskeleton.* Viruses, 2018. **10**(2): p. 1-20.

53. Roberts, K.L. and J.D. Baines, *Actin in herpesvirus infection.* Viruses, 2011. **3**(4): p. 336-346.

54. Döhner, K., et al., *Function of Dynein and Dynactin in Herpes Simplex Virus Capsid Transport.* Molecular Biology of the Cell, 2002. **13**(8): p. 2795-2809.

55. Clement, C., et al., *A novel role for phagocytosis-like uptake in herpes simplex virus entry.* The Journal of Cell Biology, 2006. **174**(7): p. 1009-1021.

56. Butcher, M., K. Raviprakash, and H.P. Ghosh, *Acid pH-induced fusion of cells by herpes simplex virus glycoproteins gB an gD.* The journal of biological chemistry, 1990. **265**(10): p. 5862-5868.

57. Nicola, A.V., A.M. McEvoy, and S.E. Straus, *Roles for endocytosis and low pH in herpes simplex virus entry into HeLa and Chinese hamster ovary cells.* Journal of virology, 2003. **77**(9): p. 5324-5332.

58. Nicola, A.V., *Herpesvirus Entry into Host Cells Mediated by Endosomal Low pH.* Traffic, 2016. **17**(9): p. 965-975.

59. Milne, R.S.B., et al., *Glycoprotein D Receptor-Dependent, Low-pH-Independent Endocytic Entry of Herpes Simplex Virus Type 1.* Journal of Virology, 2005. **79**(11): p. 6655-6663.

60. Devadas, D., et al., *Herpes Simplex Virus Internalization into Epithelial Cells Requires Na+/H+ Exchangers and p21-Activated Kinases but neither Clathrin- nor Caveolin-Mediated Endocytosis.* Journal of Virology, 2014. **88**(22): p. 13378-13394.

61. Rahn, E., et al., *Entry Pathways of Herpes Simplex Virus Type 1 into Human Keratinocytes Are Dynamin- and Cholesterol-Dependent.* PLOS ONE, 2011. **6**(10): p. 1-13.

62. Akhtar, J. and D. Shukla, *Viral entry mechanisms: cellular and viral mediators of herpes simplex virus entry.* The FEBS journal, 2009. **276**(24): p. 7228-7236.

63. Naim, B., et al., *Passive and facilitated transport in nuclear pore complexes is largely uncoupled.* The journal of biological chemistry, 2007. **282**(6): p. 3881-3888.

64. Timney, B.L., et al., *Simple rules for passive diffusion through the nuclear pore complex.* The Journal of Cell Biology, 2016. **215**(1): p. 57-76.

65. Fernandez-Martinez, J. and M.P. Rout, *Nuclear pore complex biogenesis.* Current Opinion Cell Biology, 2009. **21**(4): p. 603-612.

66. Panté, N. and M. Kann, *Nuclear pore complex is able to transport macromolecules with diameters of about 39 nm.* Molecular biology of the cell, 2002. **13**(2): p. 425-434.

67. Brown, J.C. and W.W. Newcomb, *Herpesvirus capsid assembly: insights from structural analysis.* Current Opinion in Virology, 2011. **1**(2): p. 142-149.

68. Preston, V.G., et al., *The UL25 Gene Product of Herpes Simplex Virus Type 1 Is Involved in Uncoating of the Viral Genome.* Journal of Virology, 2008. **82**(13): p. 6654-6666.

69. Ojala, P.M., et al., *Herpes simplex virus type 1 entry into host cells: reconstitution of capsid binding and uncoating at the nuclear pore complex in vitro.* Molecular and cellular biology, 2000. **20**(13): p. 4922-4931.

70. Cohen, S., S. Au, and N. Pante, *How viruses access the nucleus.* Biochimica et Biophysica Acta, 2011. **1813**(9): p. 1634-1645.

71. Brandariz-Nuñez, A., et al., *Pressure-driven release of viral genome into a host nucleus is a mechanism leading to herpes infection.* eLife, 2019. **8**: p. 1-20.

72. Jovasevic, V., L. Liang, and B. Roizman, *Proteolytic cleavage of VP1-2 is required for release of herpes simplex virus 1 DNA into the nucleus.* Journal of virology, 2008. **82**(7): p. 3311-3319.

73. Bauer, D.W., et al., *Herpes virus genome, the pressure is on.* Journal of the American chemical Society, 2013. **135**(30): p. 11216-11221.

74. Sandri-Goldin, R.M., et al., *Expression of herpes simplex virus beta and gamma genes integrated in mammalian cells and their induction by an alpha gene product.* Molecular and Cellular Biology, 1983. **3**(11): p. 2028-2044.

75. Dembowski, J.A., S.E. Dremel, and N.A. DeLuca, *Replication-Coupled Recruitment of Viral and Cellular Factors to Herpes Simplex Virus Type 1 Replication Forks for the Maintenance and Expression of Viral Genomes.* PLOS Pathogens, 2017. **13**(1): p. 1-23.

76. Lieu, P.T. and E.K. Wagner, *Two Leaky-Late HSV-1 Promoters Differ Significantly in Structural Architecture.* Virology, 2000. **272**(1): p. 191-203.

77. Che, Y.-c., L. Jiang, and Q.-h. Li, *Molecular modification of a HSV-1 protein and its associated gene transcriptional regulation.* Virologica Sinica, 2008. **23**(6): p. 394-398.

78. Harkness, J.M., M. Kader, and N.A. DeLuca, *Transcription of the herpes simplex virus 1 genome during productive and quiescent infection of neuronal and nonneuronal cells.* Journal of virology, 2014. **88**(12): p. 6847-6861.

79. Honess, R.W. and B. Roizman, *Regulation of Herpesvirus Macromolecular Synthesis I. Cascade Regulation of the Synthesis of Three Groups of Viral Proteins.* Journal of Virology, 1974. **14**(1): p. 8-19.

80. Muylaert, I. and P. Elias, *Knockdown of DNA ligase IV/XRCC4 by RNA interference inhibits herpes simplex virus type I DNA replication.* The journal of biological chemistry, 2007. **282**(15): p. 10865-10872.

81. Oh, J. and N.W. Fraser, *Temporal Association of the Herpes Simplex Virus Genome with Histone Proteins during a Lytic Infection.* Journal of Virology, 2008. **82**(7): p. 3530-3537.

82. Oh, J., et al., *Genome wide nucleosome mapping for HSV-1 shows nucleosomes are deposited at preferred positions during lytic infection.* PLOS ONE, 2015. **10**(2): p. 1-26.

83. Cliffe, A.R. and D.M. Knipe, *Herpes simplex virus ICP0 promotes both histone removal and acetylation on viral DNA during lytic infection.* Journal of Virology, 2008. **82**(24): p. 12030-12038.

84. Kent, J.R., et al., *During Lytic Infection Herpes Simplex Virus Type 1 Is Associated with Histones Bearing Modifications That Correlate with Active Transcription.* Journal of Virology, 2004. **78**(18): p. 10178-10186.

85. Liang, Y., et al., *A Novel Selective LSD1/KDM1A Inhibitor Epigenetically Blocks Herpes Simplex Virus Lytic Replication and Reactivation from Latency.* mBio, 2013. **4**(1): p. 1-9.

86. Narayanan, A., W.T. Ruyechan, and T.M. Kristie, *The coactivator host cell factor-1 mediates Set1 and MLL1 H3K4 trimethylation at herpesvirus immediate early promoters for initiation of infection.* Proceedings of the National Academy of Sciences of the United States of America, 2007. **104**(26): p. 10835-10840.

87. Weller, S.K. and D.M. Coen, *Herpes simplex viruses: mechanisms of DNA replication.* Cold Spring Harbor perspectives in biology, 2012. **4**(9): p. 1-14.

88. Muylaert, I., K.W. Tang, and P. Elias, *Replication and recombination of herpes simplex virus DNA.* The journal of biological chemistry, 2011. **286**(18): p. 15619-15624.

89. Darwish, A.S., et al., *ICP8 Filament Formation Is Essential for Replication Compartment Formation during Herpes Simplex Virus Infection.* Journal of Virology, 2016. **90**(5): p. 2561-2570.

90. Lukonis, C.J. and S.K. Weller, *Formation of herpes simplex virus type 1 replication compartments by transfection: requirements and localization to nuclear domain 10.* Journal of Virology, 1997. **71**(3): p. 2390-2399.

91. Taylor, T.J., et al., *Herpes simplex virus replication compartments can form by coalescence of smaller compartments.* Virology, 2003. **309**(2): p. 232-247.

92. Sourvinos, G. and R.D. Everett, *Visualization of parental HSV-1 genomes and replication compartments in association with ND10 in live infected cells.* The EMBO journal, 2002. **21**(18): p. 4989-4997.

93. Summers, B.C. and D.A. Leib, *Herpes simplex virus type 1 origins of DNA replication play no role in the regulation of flanking promoters.* Journal of virology, 2002. **76**(14): p. 7020-7029.

94. He, X. and I.R. Lehman, *Unwinding of a herpes simplex virus type 1 origin of replication (Ori(S)) by a complex of the viral origin binding protein and the single-stranded DNA binding protein.* Journal of virology, 2000. **74**(12): p. 5726-5728.

95. Boehmer, P.E. and I.R. Lehman, *Herpes simplex virus DNA replication.* Annual Review of Biochemistry, 1997. **66**: p. 347-384.

96. Weerasooriya, S., et al., *Herpes simplex virus 1 ICP8 mutant lacking annealing activity is deficient for viral DNA replication.* Proceedings of the National Academy of Sciences of the United States of America, 2019. **116**(3): p. 1033-1042.

97. Mahiet, C., et al., *Structural variability of the herpes simplex virus 1 genome in vitro and in vivo.* Journal of virology, 2012. **86**(16): p. 8592-8601.

98. Mohni, K.N., et al., *DNA Mismatch Repair Proteins Are Required for Efficient Herpes Simplex Virus 1 Replication.* Journal of Virology, 2011. **85**(23): p. 12241-12253.

99. Wilkinson, D.E. and S.K. Weller, *Recruitment of Cellular Recombination and Repair Proteins to Sites of Herpes Simplex Virus Type 1 DNA Replication Is Dependent on the Composition of Viral Proteins within Prereplicative Sites and Correlates with the*

Induction of the DNA Damage Response. Journal of Virology, 2004. **78**(9): p. 4783-4796.

100. Taylor, T.J. and D.M. Knipe, *Proteomics of Herpes Simplex Virus Replication Compartments: Association of Cellular DNA Replication, Repair, Recombination, and Chromatin Remodeling Proteins with ICP8.* Journal of Virology, 2004. **78**(11): p. 5856-5866.

101. Newcomb, W.W., et al., *Isolation of herpes simplex virus procapsids from cells infected with a protease-deficient mutant virus.* Journal of Virology, 2000. **74**(4): p. 1663-1673.

102. Heymann, J.B., et al., *Dynamics of herpes simplex virus capsid maturation visualized by time-lapse cryo-electron microscopy.* Nature Structural Biology, 2003. **10**(5): p. 334-341.

103. Preston, V.G., et al., *The herpes simplex virus gene UL26 proteinase in the presence of the UL26.5 gene product promotes the formation of scaffold-like structures.* The Journal of general biology, 1994. **75 (Pt 9)**: p. 2355-2366.

104. Heming, J.D., J.F. Conway, and F.L. Homa, *Herpesvirus Capsid Assembly and DNA Packaging.* Advances in Anatomy, Embryology, and Cell Biology, 2017. **223**: p. 119-142.

105. Hodge, P.D. and N.D. Stow, *Effects of mutations within the herpes simplex virus type 1 DNA encapsidation signal on packaging efficiency.* Journal of virology, 2001. **75**(19): p. 8977-8986.

106. Dutch, R.E., et al., *Herpes simplex virus type 1 recombination: role of DNA replication and viral a sequences.* Journal of virology, 1992. **66**(1): p. 277-285.

107. Beard, P.M., C. Duffy, and J.D. Baines, *Quantification of the DNA Cleavage and Packaging Proteins UL15 and UL28 in A and B Capsids of Herpes Simplex Virus Type 1.* Journal of Virology, 2004. **78**(3): p. 1367-1374.

108. Schrag, J.D., et al., *Three-dimensional structure of the HSV1 nucleocapsid.* Cell, 1989. **56**(4): p. 651-660.

109. Trus, B.L., et al., *Allosteric signaling and a nuclear exit strategy: binding of UL25/UL17 heterodimers to DNA-Filled HSV-1 capsids.* Molecular cell, 2007. **26**(4): p. 479-489.

110. Roller, R.J. and J.D. Baines, *Herpesvirus Nuclear Egress.* Advances in Anatomy, Embryology, and Cell Biology, 2017. **223**: p. 143-169.

111. Henaff, D., et al., *Analysis of the early steps of herpes simplex virus 1 capsid tegumentation.* Journal of Virology, 2013. **87**(9): p. 4895-4906.

112. Newcomb, W.W., et al., *The Primary Enveloped Virion of Herpes Simplex Virus 1: Its Role in Nuclear Egress.* mBio, 2017. **8**(3): p. 1-14.

113. Mou, F., T. Forest, and J.D. Baines, *US3 of herpes simplex virus type 1 encodes a promiscuous protein kinase that phosphorylates and alters localization of lamin A/C in infected cells.* journal of Virology, 2007. **81**(12): p. 6459-6470.

114. Park, R. and J.D. Baines, *Herpes simplex virus type 1 infection induces activation and recruitment of protein kinase C to the nuclear membrane and increased phosphorylation of lamin B.* Journal of Virology, 2006. **80**(1): p. 494-504.

115. Maruzuru, Y., et al., *Role of herpes simplex virus 1 immediate early protein ICP22 in viral nuclear egress.* Journal of Virology, 2014. **88**(13): p. 7445-7454.

116. Liu, Z., et al., *Herpes Simplex Virus 1 UL47 Interacts with Viral Nuclear Egress Factors UL31, UL34, and Us3 and Regulates Viral Nuclear Egress.* Journal of Virology, 2014. **88**(9): p. 4657-4667.

117. Klupp, B.G., et al., *Vesicle formation from the nuclear membrane is induced by coexpression of two conserved herpesvirus proteins.* Proceedings of the National Academy of Sciences of the United States of America, 2007. **104**(17): p. 7241-7246.

118. Bigalke, J.M., et al., *Membrane deformation and scission by the HSV-1 nuclear egress complex.* Nature Communications, 2014. **5**: p. 1-12.

119. Reynolds, A.E., et al., *UL31 and UL34 Proteins of Herpes Simplex Virus Type 1 Form a Complex That Accumulates at the Nuclear Rim and Is Required for Envelopment of Nucleocapsids.* Journal of Virology, 2001. **75**(18): p. 8803-8817.

120. Arii, J., et al., *ESCRT-III mediates budding across the inner nuclear membrane and regulates its integrity.* Nature Communications, 2018. **9**(1): p. 1-15.

121. Stannard, L.M., S. Himmelhoch, and S. Wynchank, *Intra-nuclear localization of two envelope proteins, gB and gD, of herpes simplex virus.* Archives of Virology, 1996. **141**(3): p. 505-524.

122. Farnsworth, A., et al., *Herpes simplex virus glycoproteins gB and gH function in fusion between the virion envelope and the outer nuclear membrane.* Proceedings of the

National Academy of Sciences of the United States of America, 2007. **104**(24): p. 10187-10192.

123. Mou, F., E. Wills, and J.D. Baines, *Phosphorylation of the U(L)31 protein of herpes simplex virus 1 by the U(S)3-encoded kinase regulates localization of the nuclear envelopment complex and egress of nucleocapsids.* Journal of Virology, 2009. **83**(10): p. 5181-5191.

124. Wisner, T.W., et al., *Herpesvirus gB-induced fusion between the virion envelope and outer nuclear membrane during virus egress is regulated by the viral US3 kinase.* Journal of Virology, 2009. **83**(7): p. 3115-3126.

125. Bigalke, J.M. and E.E. Heldwein, *Nuclear Exodus: Herpesviruses Lead the Way.* Annual review of virology, 2016. **3**(1): p. 387-409.

126. Mettenleiter, T.C., *Herpesvirus assembly and egress.* Journal of virology, 2002. **76**(4): p. 1537-1547.

127. Morrison, E.E., et al., *Differences in the intracellular localization and fate of herpes simplex virus tegument proteins early in the infection of Vero cells.* The Journal of general biology, 1998. **79 (Pt 10)**: p. 2517-2528.

128. Loret, S. and R. Lippé, *Biochemical analysis of infected cell polypeptide (ICP)0, ICP4, UL7 and UL23 incorporated into extracellular herpes simplex virus type 1 virions.* The Journal of general biology, 2012. **93**(3): p. 624-634.

129. Bucks, M.A., et al., *Herpes simplex virus type 1 tegument proteins VP1/2 and UL37 are associated with intranuclear capsids.* Virology, 2007. **361**(2): p. 316-324.

130. Farnsworth, A., K. Goldsmith, and D.C. Johnson, *Herpes Simplex Virus Glycoproteins gD and gE/gI Serve Essential but Redundant Functions during Acquisition of the Virion Envelope in the Cytoplasm.* Journal of Virology, 2003. **77**(15): p. 8481-8494.

131. Heilingloh, C.S. and A. Krawczyk, *Role of L-Particles during Herpes Simplex Virus Infection.* Frontiers in microbiology, 2017. **8**: p. 2565-2565.

132. Rixon, F.J., C. Addison, and J. McLauchlan, *Assembly of enveloped tegument structures (L particles) can occur independently of virion maturation in herpes simplex virus type 1-infected cells.* The Journal of general biology, 1992. **73 (Pt 2)**: p. 277-284.

133. Ibiricu, I., U.E. Maurer, and K. Grünewald, *Characterization of herpes simplex virus type 1 L-particle assembly and egress in hippocampal neurones by electron cryo-tomography.* Cellular microbiology, 2013. **15**(2): p. 285-291.

134. Roussel, É. and R. Lippé, *Cellular Protein Kinase D Modulators Play a Role during Multiple Steps of Herpes Simplex Virus 1 Egress.* Journal of virology, 2018. **92**(23): p. 1-15.

135. Avitabile, E., et al., *Redistribution of microtubules and Golgi apparatus in herpes simplex virus-infected cells and their role in viral exocytosis.* Journal of Virology, 1995. **69**(12): p. 7472-7482.

136. Miranda-Saksena, M., et al., *Herpes Simplex Virus Utilizes the Large Secretory Vesicle Pathway for Anterograde Transport of Tegument and Envelope Proteins and for Viral Exocytosis from Growth Cones of Human Fetal Axons.* Journal of Virology, 2009. **83**(7): p. 3187-3199.

137. Abaitua, F., et al., *Polarized cell migration during cell-to-cell transmission of herpes simplex virus in human skin keratinocytes.* Journal of virology, 2013. **87**(14): p. 7921-7932.

138. Carmichael, J.C., et al., *The HSV-1 mechanisms of cell-to-cell spread and fusion are critically dependent on host PTP1B.* PLOS Pathogens, 2018. **14**(5): p. 1-30.

139. Dingwell, K.S., et al., *Herpes simplex virus glycoproteins E and I facilitate cell-to-cell spread in vivo and across junctions of cultured cells.* Journal of Virology, 1994. **68**(2): p. 834-845.

140. Howard, P.W., et al., *Herpes simplex virus gE/gI extracellular domains promote axonal transport and spread from neurons to epithelial cells.* Journal of Virology, 2014. **88**(19): p. 11178-11186.

141. Farnsworth, A. and D.C. Johnson, *Herpes Simplex Virus gE/gI Must Accumulate in the trans-Golgi Network at Early Times and Then Redistribute to Cell Junctions To Promote Cell-Cell Spread.* Journal of Virology, 2006. **80**(7): p. 3167-3179.

142. Balan, P., et al., *An analysis of the in vitro and in vivo phenotypes of mutants of herpes simplex virus type 1 lacking glycoproteins gG, gE, gI or the putative gJ.* Journal of General Virology, 1994. **75**(6): p. 1245-1258.

143. Rizvi, S.M. and M. Raghavan, *Responses of Herpes Simplex Virus Type 1-Infected Cells to the Presence of Extracellular Antibodies: gE-Dependent Glycoprotein Capping and Enhancement in Cell-to-Cell Spread.* Journal of Virology, 2003. **77**(1): p. 701-708.

144. Han, J., et al., *Function of glycoprotein E of herpes simplex virus requires coordinated assembly of three tegument proteins on its cytoplasmic tail.* Proceedings of the National Academy of Sciences of the United States of America, 2012. **109**(48): p. 19798-19803.

145. Saied, A.A., et al., *A replication competent HSV-1(McKrae) with a mutation in the amino-terminus of glycoprotein K (gK) is unable to infect mouse trigeminal ganglia after cornea infection.* Current eye research, 2014. **39**(6): p. 596-603.

146. Avitabile, E., G. Lombardi, and G. Campadelli-Fiume, *Herpes simplex virus glycoprotein K, but not its syncytial allele, inhibits cell-cell fusion mediated by the four fusogenic glycoproteins, gD, gB, gH, and gL.* Journal of Virology, 2003. **77**(12): p. 6836-6844.

147. Striebinger, H., et al., *Subcellular trafficking and functional importance of herpes simplex virus type 1 glycoprotein M domains.* Journal of General Virology, 2015. **96**(11): p. 3313-3325.

148. Kim, I.J., et al., *Herpes simplex virus 1 glycoprotein M and the membrane-associated protein UL11 are required for virus-induced cell fusion and efficient virus entry.* Journal of Virology, 2013. **87**(14): p. 8029-8037.

149. Ren, Y., et al., *Glycoprotein M is important for the efficient incorporation of glycoprotein H-L into herpes simplex virus type 1 particles.* The Journal of general biology, 2012. **93**(Pt 2): p. 319-329.

150. Crump, C.M., et al., *Alphaherpesvirus glycoprotein M causes the relocalization of plasma membrane proteins.* The Journal of general biology, 2004. **85**(Pt 12): p. 3517-3527.

151. Baines, J.D. and B. Roizman, *The open reading frames UL3, UL4, UL10, and UL16 are dispensable for the replication of herpes simplex virus 1 in cell culture.* Journal of Virology, 1991. **65**(2): p. 938-944.

152. MacLean, C.A., L.M. Robertson, and F.E. Jamieson, *Characterization of the UL10 gene product of herpes simplex virus type 1 and investigation of its role in vivo.* Journal of General Virology, 1993. **74**(6): p. 975-983.

153. El Kasmi, I., et al., *Extended Synaptotagmin 1 Interacts with Herpes Simplex Virus 1 Glycoprotein M and Negatively Modulates Virus-Induced Membrane Fusion.* journal of virology, 2018. **92**(1): p. 1-19.

154. Hong, W., *SNAREs and traffic.* Biochimica et Biophysica Acta, 2005. **1744**(2): p. 120-144.

155. Chen, Y.A. and R.H. Scheller, *SNARE-mediated membrane fusion.* Nature Reviews Molecular Cell Biology, 2001. **2**(2): p. 98-106.

156. Ungermann, C. and D. Langosch, *Functions of SNAREs in intracellular membrane fusion and lipid bilayer mixing.* Journal of Cell Science, 2005. **118**(17): p. 3819-3828.

157. Wong, S.H., et al., *Endobrevin, a Novel Synaptobrevin/VAMP-Like Protein Preferentially Associated with the Early Endosome.* molecular biology of the cell, 1998. **9**(6): p. 1549-1563.

158. Schiavo, G., et al., *Binding of the synaptic vesicle v-SNARE, synaptotagmin, to the plasma membrane t-SNARE, SNAP-25, can explain docked vesicles at neurotoxin-treated synapses.* Proceedings of the National Academy of Sciences of the United States of America, 1997. **94**(3): p. 997-1001.

159. Gerst, J.E., *SNAREs and SNARE regulators in membrane fusion and exocytosis.* Cellular and Molecular Life Sciences, 1999. **55**(5): p. 707-734.

160. Saheki, Y. and P. De Camilli, *The Extended-Synaptotagmins.* Biochimica et biophysica acta, 2017. **1864**(9): p. 1490-1493.

161. Herdman, C. and T. Moss, *Extended-Synaptotagmins (E-Syts); the extended story.* pharmacological research, 2016. **107**: p. 48-56.

162. Südhof, T.C., *Calcium control of neurotransmitter release.* Cold Spring Harbor perspectives in biology, 2012. **4**(1): p. 1-12.

163. Chapman, E.R., *How does synaptotagmin trigger neurotransmitter release?* Annual Review of Biochemistry, 2008. **77**: p. 615-641.

164. Min, S.W., W.P. Chang, and T.C. Sudhof, *E-Syts, a family of membranous Ca2+-sensor proteins with multiple C2 domains.* Proceedings of the National Academy of Sciences of the United States of America, 2007. **104**(10): p. 3823-3828.

165. Reinisch, K.M. and P. De Camilli, *SMP-domain proteins at membrane contact sites: Structure and function.* Biochimica et Biophysica Acta, 2016. **1861**(8 Pt B): p. 924-927.

166. Yu, H., et al., *Extended synaptotagmins are Ca2+-dependent lipid transfer proteins at membrane contact sites.* Proceedings of the National Academy of Sciences of the United States of America, 2016. **113**(16): p. 4362-4367.

167. Saheki, Y., et al., *Control of plasma membrane lipid homeostasis by the extended synaptotagmins.* Nature Cell Biology, 2016. **18**: p. 504-515.

168. Chang, C.L. and J. Liou, *Homeostatic regulation of the PI(4,5)P2-Ca(2+) signaling system at ER-PM junctions.* Biochimica et Biophysica Acta, 2016. **1861**(8 Pt B): p. 862-873.

169. Idevall-Hagren, O., et al., *Triggered Ca2+ influx is required for extended synaptotagmin 1-induced ER-plasma membrane tethering.* EMBO J, 2015. **34**(17): p. 2291-305.

170. Bian, X., Y. Saheki, and P. De Camilli, *Ca(2+) releases E-Syt1 autoinhibition to couple ER-plasma membrane tethering with lipid transport.* The EMBO journal, 2018. **37**(2): p. 219-234.

171. Subedi, K.P., H.L. Ong, and I.S. Ambudkar, *Assembly of ER-PM Junctions: A Critical Determinant in the Regulation of SOCE and TRPC1*, in *Membrane Dynamics and Calcium Signaling*, J. Krebs, Editor. 2017, Springer International Publishing: Cham. p. 253-276.

172. Chang, C.-L., Y.-J. Chen, and J. Liou, *ER-plasma membrane junctions: Why and how do we study them?* Biochimica et Biophysica Acta, 2017. **1864**(9): p. 1494-1506.

173. Prakriya, M. and R.S. Lewis, *Store-Operated Calcium Channels.* Physiological reviews, 2015. **95**(4): p. 1383-1436.

174. Pinton, P., et al., *Calcium and apoptosis: ER-mitochondria Ca2+ transfer in the control of apoptosis.* Oncogene, 2008. **27**(50): p. 6407-6418.

175. Liu, Q.-H., et al., *Membrane depolarization causes a direct activation of G protein-coupled receptors leading to local Ca2+ release in smooth muscle.* Proceedings of the National Academy of Sciences of the United States of America, 2009. **106**(27): p. 11418-11423.

176. Chen, Y.-F., et al., *Calcium store sensor stromal-interaction molecule 1-dependent signaling plays an important role in cervical cancer growth, migration, and angiogenesis.* Proceedings of the National Academy of Sciences of the United States of America, 2011. **108**(37): p. 15225-15230.

177. Pinton, P., T. Pozzan, and R. Rizzuto, *The Golgi apparatus is an inositol 1,4,5-trisphosphate-sensitive Ca2+ store, with functional properties distinct from those of the endoplasmic reticulum.* The EMBO Journal, 1998. **17**(18): p. 5298-5308.

178. Galione, A. and G.C. Churchill, *Interactions between calcium release pathways: multiple messengers and multiple stores.* Cell Calcium, 2002. **32**(5): p. 343-354.

179. Giorgi, C., S. Marchi, and P. Pinton, *The machineries, regulation and cellular functions of mitochondrial calcium.* Nature Reviews Molecular Cell Biology, 2018. **19**(11): p. 713-730.

180. Kang, F., et al., *E-syt1 Re-arranges STIM1 Clusters to Stabilize Ring-shaped ER-PM Contact Sites and Accelerate Ca2+ Store Replenishment.* Scientific Reports, 2019. **9**(1): p. 1-11.

181. Bagur, R. and G. Hajnóczky, *Intracellular Ca(2+) Sensing: Its Role in Calcium Homeostasis and Signaling.* Molecular cell, 2017. **66**(6): p. 780-788.

182. Putney, J.W. and T. Tomita, *Phospholipase C signaling and calcium influx.* Advances in biological regulation, 2012. **52**(1): p. 152-164.

183. Guillon, G., et al., *Mechanisms of phospholipase C activation: a comparison with the adenylate cyclase system.* Biochimie, 1987. **69**(4): p. 351-363.

184. Fukami, K., et al., *Phospholipase C is a key enzyme regulating intracellular calcium and modulating the phosphoinositide balance.* Progress in lipid research, 2010. **49**(4): p. 429-437.

185. Manford, A.G., et al., *ER-to-plasma membrane tethering proteins regulate cell signaling and ER morphology.* Developmental cell, 2012. **23**(6): p. 1129-1140.

186. Micaroni, M., *Calcium around the Golgi apparatus: implications for intracellular membrane trafficking.* Advances in experimental medecine and biolgy, 2012. **740**: p. 439-460.

187. Takahara, T., et al., *The calcium-binding protein ALG-2 regulates protein secretion and trafficking via interactions with MISSL and MAP1B proteins.* The journal of biological chemistry, 2017. **292**(41): p. 17057-17072.

188. Zheng, K., et al., *Calcium-signal facilitates herpes simplex virus type 1 nuclear transport through slingshot 1 and calpain-1 activation.* Virus research, 2014. **188**: p. 32-37.

189. Cheshenko, N., et al., *Herpes simplex virus triggers activation of calcium-signaling pathways.* The Journal of Cell Biology, 2003. **163**(2): p. 283-293.

190. Cheshenko, N., et al., *Multiple receptor interactions trigger release of membrane and intracellular calcium stores critical for herpes simplex virus entry.* Molecular biology of the cell, 2007. **18**(8): p. 3119-3130.

191. Register, R.B. and J.A. Shafer, *A facile system for construction of HSV-1 variants: site directed mutation of the UL26 protease gene in HSV-1.* Journal of Virological Methods, 1996. **57**(2): p. 181-193.

192. Kobayashi, R., et al., *Herpes Simplex Virus 1 Small Capsomere-Interacting Protein VP26 Regulates Nucleocapsid Maturation.* Journal of Virology, 2017. **91**(18): p. 1-18.

193. Giordano, F., et al., *PI(4,5)P(2)-dependent and Ca(2+)-regulated ER-PM interactions mediated by the extended synaptotagmins.* Cell, 2013. **153**(7): p. 1494-1509.

194. Tsien, R.Y., *New calcium indicators and buffers with high selectivity against magnesium and protons: design, synthesis, and properties of prototype structures.* Biochemistry, 1980. **19**(11): p. 2396-2404.

195. Tsien, R.Y., *A non-disruptive technique for loading calcium buffers and indicators into cells.* Nature, 1981. **290**(5806): p. 527-528.

196. Tymianski, M., et al., *Mechanism of action and persistence of neuroprotection by cell-permeant Ca2+ chelators.* Jounal of Cerebral Blood Flow and Metabolism, 1994. **14**(6): p. 911-923.

197. Vay, L., et al., *Modulation of Ca(2+) release and Ca(2+) oscillations in HeLa cells and fibroblasts by mitochondrial Ca(2+) uniporter stimulation.* The Journal of physiology, 2007. **580**(Pt 1): p. 39-49.

198. Crawford, J.R. and B.S. Jacobson, *Extracellular calcium regulates HeLa cell morphology during adhesion to gelatin: role of translocation and phosphorylation of cytosolic phospholipase A2.* Molecular biology of the cell, 1998. **9**(12): p. 3429-3443.

199. Nicholson, P., et al., *Localization of the herpes simplex virus type 1 major capsid protein VP5 to the cell nucleus requires the abundant scaffolding protein VP22a.* The Journal of general biology, 1994. **75 (Pt 5)**: p. 1091-1099.

200. Ruhge, L.L., et al., *The Apical Region of the Herpes Simplex Virus Major Capsid Protein Promotes Capsid Maturation.* Journal of Virology, 2018. **92**(18): p. 1-16.

201. Mingo, R.M., et al., *Replication of Herpes Simplex Virus: Egress of Progeny Virus at Specialized Cell Membrane Sites.* Journal of Virology, 2012. **86**(13): p. 7084-7097.

202. Rémillard-Labrosse, G., G. Guay, and R. Lippé, *Reconstitution of Herpes Simplex Virus Type 1 Nuclear Capsid Egress In Vitro.* Journal of Virology, 2006. **80**(19): p. 9741-9753.

203. Liu, C. and T.E. Hermann, *Characterization of ionomycin as a calcium ionophore.* The journal of biological chemistry, 1978. **253**(17): p. 5892-5894.

204. Honess, R.W. and D.H. Watson, *Herpes simplex virus resistance and sensitivity to phosphonoacetic acid.* Journal of Virology, 1977. **21**(2): p. 584-600.

205. Overby, L.R., et al., *Inhibition of herpes simplex virus replication by phosphonoacetic acid.* Antimicrobial agents and chemotherapy, 1974. **6**(3): p. 360-365.

206. Coe, H. and M. Michalak, *Calcium binding chaperones of the endoplasmic reticulum.* General physiology and biophysics, 2009. **28**: p. 96-103.

207. Williams, J.A., et al., *Role of intracellular calcium in proteasome inhibitor-induced endoplasmic reticulum stress, autophagy, and cell death.* Pharmaceutical research, 2013. **30**(9): p. 2279-2289.

208. Bravo, R., et al., *Endoplasmic reticulum and the unfolded protein response: dynamics and metabolic integration.* International review of cell and molecular biology, 2013. **301**: p. 215-290.

209. Li, S., L. Kong, and X. Yu, *The expanding roles of endoplasmic reticulum stress in virus replication and pathogenesis.* Critical reviews in microbiology, 2015. **41**(2): p. 150-164.

210. Burnett, H.F., et al., *Herpes simplex virus-1 disarms the unfolded protein response in the early stages of infection.* Cell stress & chaperones, 2012. **17**(4): p. 473-483.

211. Mulvey, M., et al., *Regulation of eIF2alpha phosphorylation by different functions that act during discrete phases in the herpes simplex virus type 1 life cycle.* Journal of Virology, 2003. **77**(20): p. 10917-10928.

212. Okudera, M., et al., *Effect of ionomycin on interaction of calnexin with vesicular stomatitis virus glycoprotein is cell type-specific.* Journal of oral science, 2015. **57**(4): p. 305-312.

213. Vallbracht, M., et al., *Functional Role of N-Linked Glycosylation in Pseudorabies Virus Glycoprotein gH.* Journal of Virology, 2018. **92**(9): p. 1-18.

214. Rider, P.J.F., et al., *Cysteines and N-Glycosylation Sites Conserved among All Alphaherpesviruses Regulate Membrane Fusion in Herpes Simplex Virus 1 Infection.* Journal of Virology, 2017. **91**(21): p. 1-14.

215. Compton, T. and R.J. Courtney, *Evidence for post-translational glycosylation of a nonglycosylated precursor protein of herpes simplex virus type 1.* Journal of Virology, 1984. **52**(2): p. 630-637.

216. Luo, S., et al., *Contribution of N-linked glycans on HSV-2 gB to cell–cell fusion and viral entry.* Virology, 2015. **483**: p. 72-82.

217. Chen, X., R. Cao, and W. Zhong, *Host Calcium Channels and Pumps in Viral Infections.* Cells, 2019. **9**(1): p. 1-13.

218. *Microinjection of Ca++-calmodulin causes a localized depolymerization of microtubules.* The Journal of Cell Biology, 1983. **97**(6): p. 1918-1924.

219. O'Brien, E.T., E.D. Salmon, and H.P. Erickson, *How calcium causes microtubule depolymerization.* Cell Motility, 1997. **36**(2): p. 125-135.

220. Dolan, M.T., C.G. Reid, and H.P. Voorheis, *Calcium ions initiate the selective depolymerization of the pellicular microtubules in bloodstream forms of Trypanosoma brucei.* Journal of Cell Science, 1986. **80**(1): p. 123-140.

221. Parkinson, K., et al., *Calcium-dependent regulation of Rab activation and vesicle fusion by an intracellular P2X ion channel.* Nature cell biology, 2014. **16**(1): p. 87-98.

222. Raza, S., et al., *Role of Rab GTPases in HSV-1 infection: Molecular understanding of viral maturation and egress.* Microbial Pathogenesis, 2018. **118**: p. 146-153.

223. Sun, L., et al., *Cyclic GMP-AMP Synthase Is a Cytosolic DNA Sensor That Activates the Type I Interferon Pathway.* Science, 2013. **339**(6121): p. 786-791.

224. Li, T., et al., *Acetylation modulates cellular distribution and DNA sensing ability of interferon-inducible protein IFI16.* Proceedings of the National Academy of Sciences of the United States of America, 2012. **109**(26): p. 10558-10563.

225. Wu, J., et al., *Cyclic GMP-AMP Is an Endogenous Second Messenger in Innate Immune Signaling by Cytosolic DNA.* Science, 2013. **339**(6121): p. 826-830.

226. Su, C., G. Zhan, and C. Zheng, *Evasion of host antiviral innate immunity by HSV-1, an update.* Virology journal, 2016. **13**: p. 38-47.

227. Emeny, J.M. and M.J. Morgan, *Regulation of the interferon system: evidence that Vero cells have a genetic defect in interferon production.* The Journal of general virology, 1979. **43**(1): p. 247-252.

228. Osada, N., et al., *The genome landscape of the african green monkey kidney-derived vero cell line.* DNA research : an international journal for rapid publication of reports on genes and genomes, 2014. **21**(6): p. 673-683.

229. Richardson, B.A. and J. Overbaugh, *Basic statistical considerations in virological experiments.* Journal of virology, 2005. **79**(2): p. 669-676.

230. Mishra, P., et al., *Application of student's t-test, analysis of variance, and covariance.* Annals of cardiac anaesthesia, 2019. **22**(4): p. 407-411.